NASA/TM—2012-217112

Performance Analysis of a NASA Integrated Network Array

James A. Nessel
Glenn Research Center, Cleveland, Ohio

May 2012

NASA STI Program . . . in Profile

Since its founding, NASA has been dedicated to the advancement of aeronautics and space science. The NASA Scientific and Technical Information (STI) program plays a key part in helping NASA maintain this important role.

The NASA STI Program operates under the auspices of the Agency Chief Information Officer. It collects, organizes, provides for archiving, and disseminates NASA's STI. The NASA STI program provides access to the NASA Aeronautics and Space Database and its public interface, the NASA Technical Reports Server, thus providing one of the largest collections of aeronautical and space science STI in the world. Results are published in both non-NASA channels and by NASA in the NASA STI Report Series, which includes the following report types:

- TECHNICAL PUBLICATION. Reports of completed research or a major significant phase of research that present the results of NASA programs and include extensive data or theoretical analysis. Includes compilations of significant scientific and technical data and information deemed to be of continuing reference value. NASA counterpart of peer-reviewed formal professional papers but has less stringent limitations on manuscript length and extent of graphic presentations.

- TECHNICAL MEMORANDUM. Scientific and technical findings that are preliminary or of specialized interest, e.g., quick release reports, working papers, and bibliographies that contain minimal annotation. Does not contain extensive analysis.

- CONTRACTOR REPORT. Scientific and technical findings by NASA-sponsored contractors and grantees.

- CONFERENCE PUBLICATION. Collected papers from scientific and technical conferences, symposia, seminars, or other meetings sponsored or cosponsored by NASA.

- SPECIAL PUBLICATION. Scientific, technical, or historical information from NASA programs, projects, and missions, often concerned with subjects having substantial public interest.

- TECHNICAL TRANSLATION. English-language translations of foreign scientific and technical material pertinent to NASA's mission.

Specialized services also include creating custom thesauri, building customized databases, organizing and publishing research results.

For more information about the NASA STI program, see the following:

- Access the NASA STI program home page at *http://www.sti.nasa.gov*

- E-mail your question via the Internet to *help@sti.nasa.gov*

- Fax your question to the NASA STI Help Desk at 443–757–5803

- Telephone the NASA STI Help Desk at 443–757–5802

- Write to:
  NASA Center for AeroSpace Information (CASI)
  7115 Standard Drive
  Hanover, MD 21076–1320

NASA/TM—2012-217112

Performance Analysis of a NASA Integrated Network Array

James A. Nessel
Glenn Research Center, Cleveland, Ohio

National Aeronautics and
Space Administration

Glenn Research Center
Cleveland, Ohio 44135

May 2012

Level of Review: This material has been technically reviewed by technical management.

Available from

NASA Center for Aerospace Information
7115 Standard Drive
Hanover, MD 21076–1320

National Technical Information Service
5301 Shawnee Road
Alexandria, VA 22312

Available electronically at http://www.sti.nasa.gov

Executive Summary

The Space Communications and Navigation (SCaN) Program is planning to integrate its individual networks into a unified network which will function as a single entity to provide services to user missions. This integrated network architecture is expected to provide SCaN customers with the capabilities to seamlessly use any of the available SCaN assets to support their missions and allow the SCaN Program to optimize the application of its assets to efficiently meet the collective needs of Agency missions. One potential optimal application of these assets, based on this envisioned architecture, is that of arraying across network assets to significantly enhance data rates and/or link availabilities.

As such, the goal of this study is to determine if or to what extent inter-network antenna arraying in the next generation integrated network architecture will enhance space communications performance, particularly with respect to link margin improvement in transmit and receive.

The results presented in this report thus address the following question:

What theoretical performance benefits can be realized by arraying antenna elements within the framework of a single integrated NASA network?

The key assumptions made in this preliminary analysis include:

- Utilization of current state-of-practice Deep Space Network (DSN), Near Earth Network (NEN), and Space Network (SN) antenna asset limitations (e.g., gain, noise temperature, transmitter power).
- Common spectrum usage amongst all antenna assets (X-band frequency used in simulations).
- Line-of-Sight (LOS) links from ground to space assets down to 10° elevation angles.

From the results of the analysis, the following important conclusions addressing theoretical SCaN Integrated Network Array performance are derived:

- A full SCaN Integrated Network Array (DSN+NEN+SN) provides no improvement in overall receive array performance and marginal improvement in transmit arraying performance, relative to DSN arraying alone. In other words, if the DSN element is being utilized in space communications, the addition of the NEN and SN elements into a total network array increases complexity with no realizable improvement in data rate and link availability.
- Intra-network arraying, on the other hand, provides significant improvement for most to all transmit and receive arraying scenarios, relative to the current state of practice of single aperture usage. For given orbital scenarios, improvements of a minimum of 3 to 10 dB in G/T and 5 to 10 dB in EIRP is realizable. All things being equal, this will directly translate to a minimum of double to an order of magnitude improvement in data rate capabilities.

Based on these findings, it is recommended that NASA proceed with the network antenna arraying concept, but with a focus on a network-centric approach, as opposed to a single NASA Integrated Network Array. This will drastically reduce complexity in implementation and maximize return on investment for upcoming NASA network upgrades.

Performance Analysis of a NASA Integrated Network Array

James A. Nessel
National Aeronautics and Space Administration
Glenn Research Center
Cleveland, Ohio 44135

1.0 SCaN Network Architecture Evolution

The current NASA space communications architecture, shown pictorially in Figure 1, is comprised of three operational networks that collectively and effectively provide communications services to supported user missions through an amalgam of space-based and ground-based assets:

- **Space Network (SN)**.—Constellation of geosynchronous relays (Tracking and Data Relay Satellites [TDRS]) and associated ground systems primarily providing transponder services for low Earth orbiting (LEO) spacecraft
- **Deep Space Network (DSN)**.—Large aperture ground stations spaced around the world providing continuous coverage of satellites from geosynchronous Earth orbit (GEO) to the edge of our solar system
- **Near Earth Network (NEN)**.—NASA, commercial, and partner ground stations and integration systems providing space communications and tracking services to lunar, orbital and suborbital missions

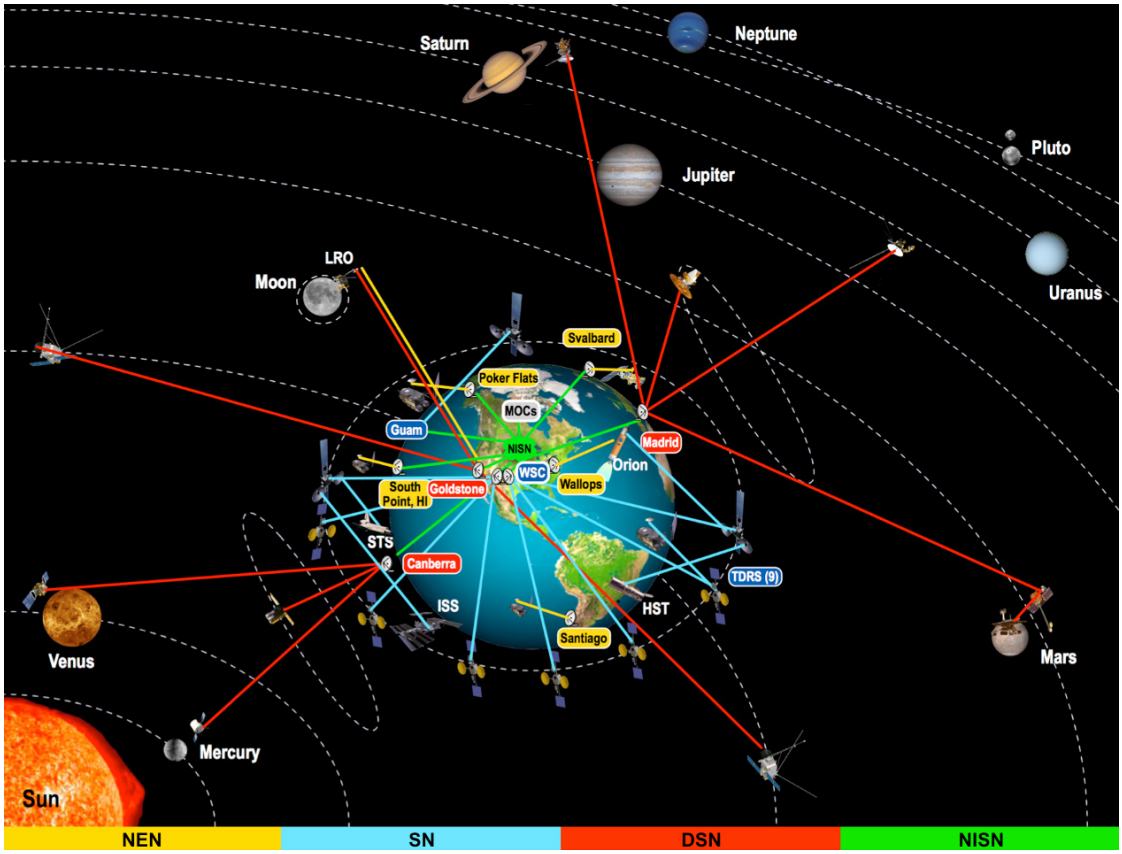

Figure 1.—Pictorial representation of current NASA communications architecture.[1]

[1]Space Communications and Integration (SCaN) Integrated Network Architecture Definition Document (ADD) Vol. 1 Executive Summary, Rev. 1, January 4, 2010

These networks are each optimized to support user missions in specific operational domains (ranging from near Earth to deep space) where the communications and tracking requirements are quite distinct. Thus, the present architecture is very capable, but is also complex because of the heterogeneous nature of the network assets and the lack of consistent service offerings, interfaces, and interoperability. The inherent complexity is attributable to the fact that each network, i.e., SN, NEN, and DSN, has been evolving independently for as long as four decades on their own respective paths.

The vision for the future SCaN architecture is to build and maintain a scalable and integrated infrastructure that provides comprehensive, robust, and cost effective space communications services at order-of-magnitude higher data rates to enable NASA's science and exploration missions, as depicted in Figure 2. To realize this, the current SCaN networks will evolve into a single integrated network by implementing an architecture that includes a consistent suite of international standards, interfaces and protocols. While the different operating domains and unique customer needs will still necessitate some distinct capabilities, the integrated network will use common crosscutting standards and implementations to the greatest extent possible. An integrated network operations and management function will serve as the interface for all NASA SCaN network customers, which lends itself to advanced operational technologies such as inter-network arraying.

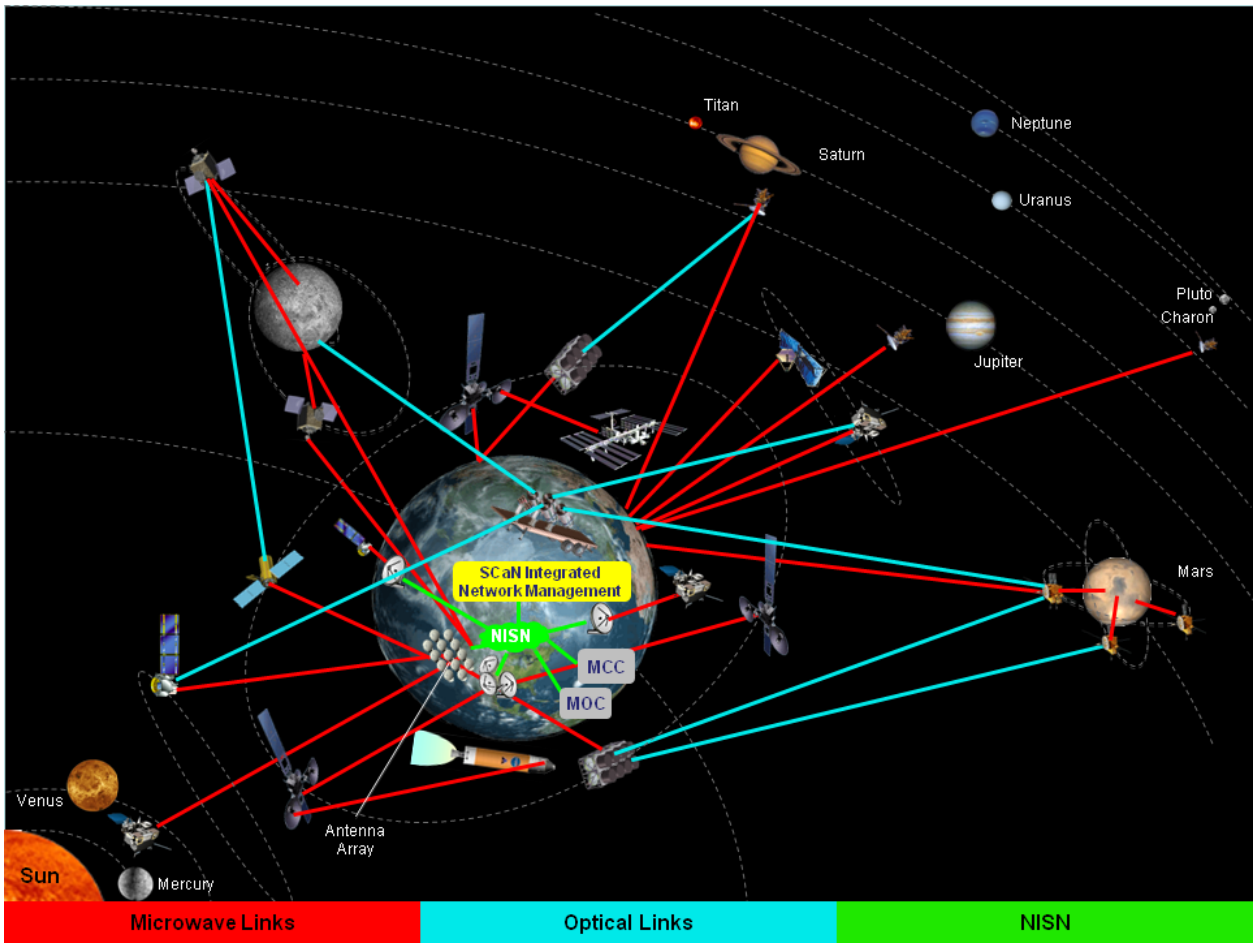

Figure 2.—SCaN Notional Integrated Network Architecture (circa 2025).[1]

2.0 SCaN Integrated Network Array

The concept behind the Integrated Network Array is built upon the premise that its realization, though relatively complex to implement, would represent the optimal performance of a fully integrated SCaN communications system. By arraying all available assets in view of a particular spacecraft, orders of magnitude increase in system gain can be readily achieved. And, based upon the requirements determined for the future SCaN network architecture, NASA is well-positioned to begin considering the implementation of an Integrated Network Array technology development plan and architecture.

The following section provides an analysis of the predicted performance of the SCaN Integrated Network Array for receive and transmit applications. Theoretical array performance, in terms of Gain over System Temperature ratio (G/T) and Effective Isotropic Radiated Power (EIRP), are derived to lay the foundation for a simulated scenario of G/T and EIRP improvement as a function of orbital distance and time of day.

2.1 Theoretical Performance of an Integrated Network Array

The approach taken in determining performance benefits of an integrated network arraying architecture is to quantify the improvement in the realizable link margin when considering the receive array (G/T) and the transmit array scenarios (EIRP). The full derivation of these terms in an array environment is provided in Appendices A and B, respectively, and a summary of the pertinent results are presented below.

2.1.1 SCaN Integrated Network Array Performance: Assumptions

Line of sight (LOS) visibility analysis using STK simulation software was performed for an arbitrary equatorial orbiting spacecraft at various orbital distances (see Appendix F). Though these quantitative results are limited to this particular scenario (due to the specific geometry), the general conclusions derived from this analysis are applicable to all arraying situations, since the arraying process is unchanged.

All simulations performed herein are conducted under the following assumptions:

- Utilization of current Deep Space Network (DSN), Near Earth Network (NEN), and Space Network (SN) antenna asset limitations (in terms of gain, system noise temperature, transmitter power). A summary of these parameters for each DSN, NEN, and SN antenna is provided in Appendices C, D, and E, respectively.
- Common spectrum usage amongst all antenna assets (X-band operational frequency: 8.4 GHz).
- LOS links from ground to space assets down to minimum 10° elevation angles.
- Omni-directional antenna at spacecraft.
- Satellite orbit at Earth equatorial plane from low Earth orbit (LEO) to lunar orbital distances.
- Only consider ground station antennas of diameter >10-m (smaller aperture antennas contribute marginal improvement in array performance).
- Include the potential use of SN ground segment antennas for receive/transmit arraying[2].

2.1.2 SCaN Integrated Network Array Performance: Receive Array

For a receive arraying scenario, the fundamental figure of merit in determining array sensitivity is a large G/T. For an array of N antennas, each with individual antenna element gain, G_i, and system noise temperature, T_i, the improvement in arraying gain is given by,

[2]Note: this scenario is likely not realizable in the future SCaN Integrated Network architecture, but included in the simulation to determine if impact on array performance is significant.

$$\left.\frac{G}{T}\right|_{array} = \frac{\left(\sum_{i=1}^{N} \alpha_i \sqrt{G_i}\right)^2}{\sum_{i=1}^{N} \alpha_i^2 T_i + T_{B\_eff}} \tag{2.1}$$

where α_i is the individual element amplitude weighting factor (whose optimal value is derived in Appendix A), and T_{B_eff} is the correlated effective sky brightness temperature common to the array elements. From this relationship, several intuitive conclusions can be drawn regarding the sensitivity of a large array. Considering a simplistic case in which all the antenna elements are identical in gain and system noise temperature, the arraying G/T, with optimal weights, can be simplified to

$$\left.\frac{G}{T}\right|_{array} = N\left(\frac{G}{T}\right) \tag{2.2}$$

A plot of the improvement in array G/T as a function of the number of identical elements added to the array is shown in Figure 3. From Figure 3, it is obvious that as we continue to add more elements, the improvement in the G/T of the array, relative to a single element, is marginalized rather quickly, due to the linear function of array size. In fact, by the time the array has grown to 10 elements, the enhancement in G/T by an additional element is only 0.4 dB. Keep in mind that this is for the case of 10 *identical* elements. For elements of varying aperture size and system noise temperature, this improvement will be dominated by the most sensitive receiver and the addition of less sensitive elements will have little to no effect. This was evident in the results of the simulation for the SCaN Integrated Network Array performance discussed below.

Appendix F provides the STK results for individual ground station visibility of an equatorial orbiting spacecraft at various orbital distances throughout a 24 hr period. Figure 4 shows the resulting SCaN Integrated Network Array G/T performance for spacecraft orbits from LEO (1,000 km) to extra-lunar orbit (500,000 km) at a fixed reference time, 16:00 UTC. Figure 5 shows the G/T improvement over the course of the full 24-hr period for a fixed sub-lunar orbit (200,000 km), relative to single aperture DSN or NEN coverage.

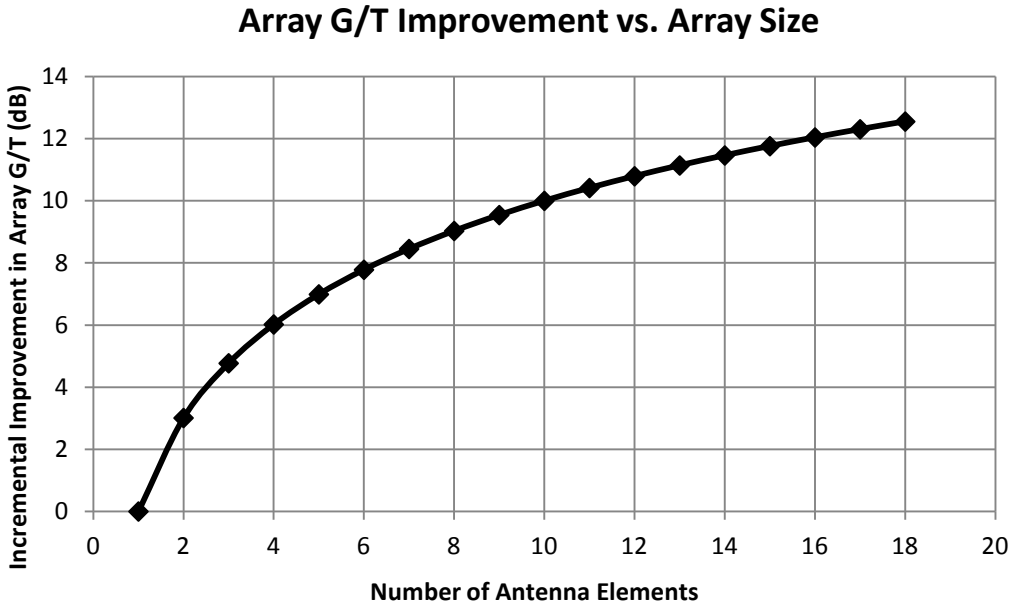

Figure 3.—Plot of incremental improvement in array G/T performance as more identical elements are added to an antenna array. Improvement is relative to a single antenna element.

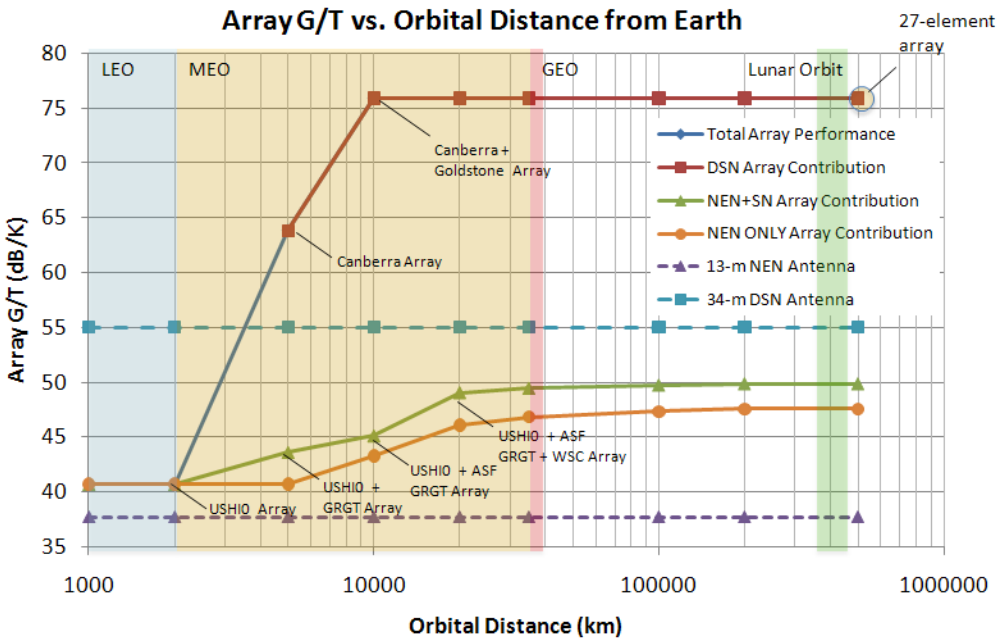

Figure 4.—SCaN Integrated Network Array G/T performance for varying equatorial orbits. Simulation time reference is fixed at 16:00 UTC. Array element labels can be referenced in Appendices C to E.

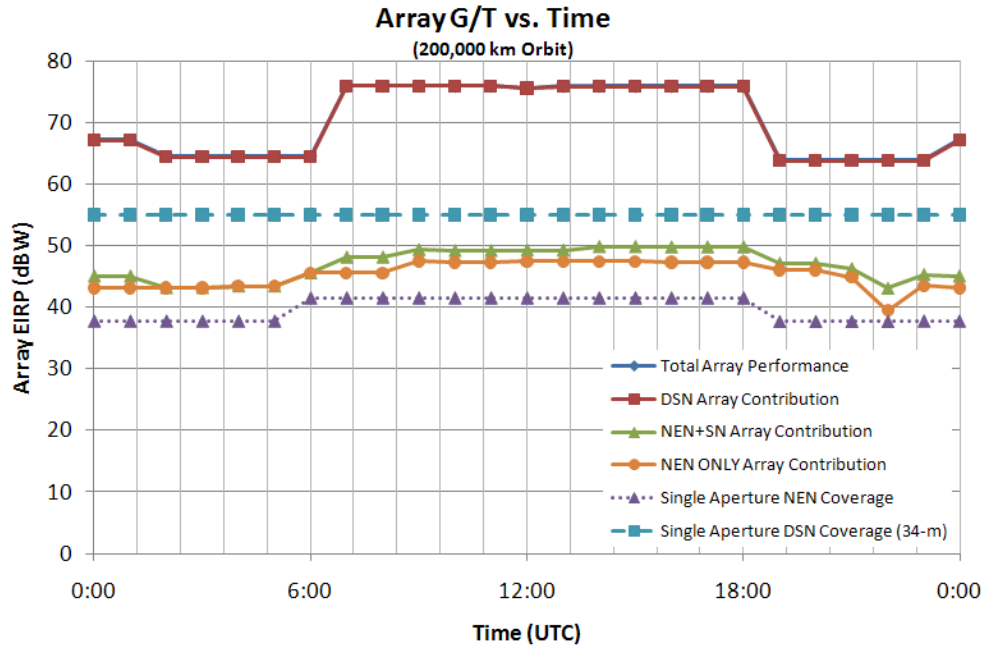

Figure 5.—SCaN Integrated Network Array G/T performance for a 200,000 km orbit over a 24-hr period.

Several key conclusions can be derived from the results of these figures:

1. As orbital distance is increased from LEO orbit to beyond lunar orbit, the availability of visible NASA ground station assets increases. For this particular scenario, a maximum of 27 NASA ground station communications assets become visible to an equatorial orbiting spacecraft (at time reference, 16:00 UTC with a duration of 1 hr).

2. Total SCaN Integrated Network Array G/T performance (solid blue line) is dominated by the G/T of the DSN elements of the array (solid red line). In other words, addition of the NEN and SN ground station elements in the total array performance provides ***no improvement in total array performance***. This is consistent with expected results, as the DSN antenna elements are significantly more sensitive than either of the NEN or SN antennas.
3. Within a given network (*i.e.*, the DSN array, NEN array, or the combined NEN+SN array), array G/T performance is significantly enhanced over the state-of-practice use of a single antenna element.
    - Arraying of all Canberra DSN assets (two 34-m and one 70-m antenna) indicates an approximate 10-dB improvement in G/T relative to a single 34-m DSN antenna (dashed blue line), but only a 1-dB improvement in G/T relative to a single 70-m DSN antenna (not shown in figure).
    - For periods of time when multiple DSN sites are in view of a spacecraft (i.e., Canberra and Goldstone for 0.5 to 1 hr in this particular scenario), DSN arraying improves G/T by more than 20 dB relative to a single 34-m DSN antenna, or a 12-dB improvement relative to a single 70-m DSN antenna.
    - NEN arraying (solid orange line) can provide 3 to 10 dB improvement in G/T over the state-of-practice implementation of a single 13-m aperture antenna (dotted purple line).
    - For an integrated NEN+SN ground station array (solid green line), an additional 3-dB improvement in G/T over solely NEN arraying is realizable for most orbital arrangements.
4. For a given day, DSN arraying improves G/T by a minimum of 10 dB relative to a single 34-m aperture antenna, while NEN arraying provides an approximate 5 dB improvement over state of practice. Integrating an NEN+SN array provides a maximum 3 dB excess margin.

2.1.3 SCaN Integrated Network Array Performance: Transmit Array

In a transmit arraying scenario, the fundamental figure of merit in determining array performance is the EIRP. For an array of N antennas, each with individual antenna element gain, G_n, and transmit power, P_m, the total array EIRP is given by the product of the sums of the individual antenna element gains and transmit powers (see Appendix B for full derivation).

$$EIRP_{array} = G_{array} \sum_{m=1}^{N} P_m = \left[\sum_{n=1}^{N} G_n\right]\left[\sum_{m=1}^{N} P_m\right] \tag{2.3}$$

Let us consider the simple case of an array of N identical antenna elements, each transmitting the same power, P. This assumption gives us the well-known N^2 improvement in EIRP due to coherent arraying.

$$EIRP_{array} = N^2 GP \tag{2.4}$$

A plot of the incremental improvement in EIRP as more elements are added to an array demonstrates the dramatic enhancements possible (see Figure 6). Though theoretically possible to increase without bound, the improvement in EIRP due to additional antenna elements begins to show marginal improvement at 20 elements, only adding approximately 0.4 dB/element as the array size increases beyond this point. This is inherently due to the square law relationship with array size. Further, for non-identical elements in an array, the increase in EIRP will be dominated by the largest individual EIRP contributors. Compared to the receive scenario derived above, uplink arraying provides much larger improvements in array performance, due to the N^2 relation to array size.

For the same scenarios described in the receive case, the transmit case is now investigated. Figure 7 shows the improvement in arraying EIRP at the same reference time, 16:00 UTC, for various orbits. Figure 8 shows the improvement in arraying EIRP at a fixed sub-lunar orbit of 200,000 km over the course of 24 hr. Notice, from Figure 7, that integrating the NEN+SN array together provides a much more

drastic increase in array performance, relative to the NEN ONLY array. This is primarily due to the fact that the transmit powers of the SN ground segment provides an additional 3 kW of power/antenna element, which is much larger than currently available in the NEN infrastructure.

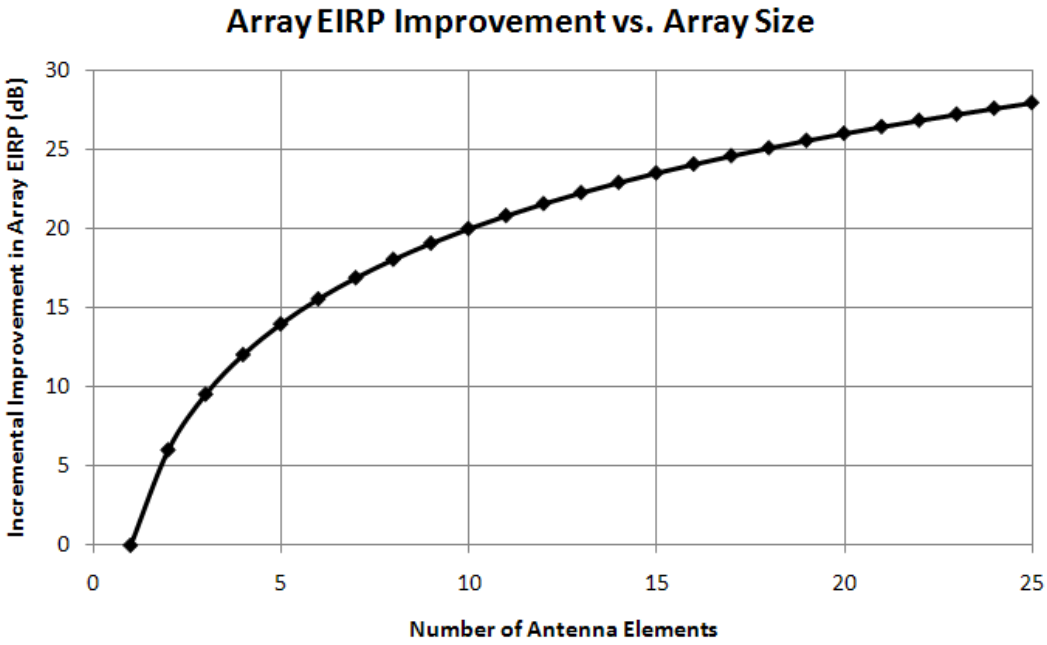

Figure 6.—Plot of incremental improvement in array EIRP performance as more identical elements are added to an antenna array. Improvement is relative to a single antenna element.

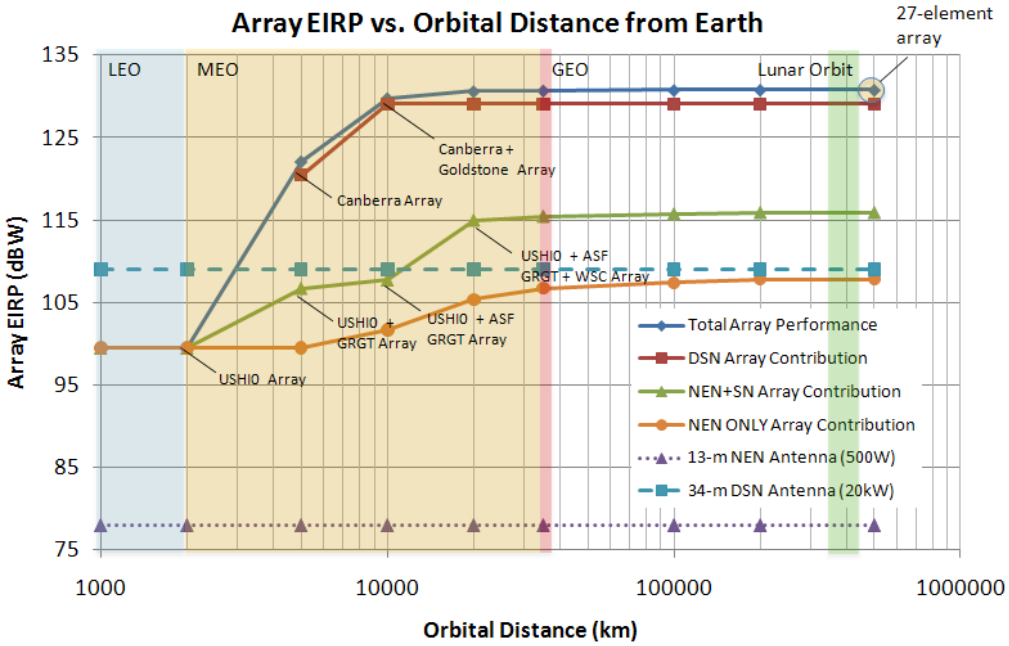

Figure 7.—SCaN Integrated Network Array EIRP performance for varying equatorial orbits. Simulation time reference is fixed at 16:00 UTC. Array element labels can be referenced in Appendices C to E.

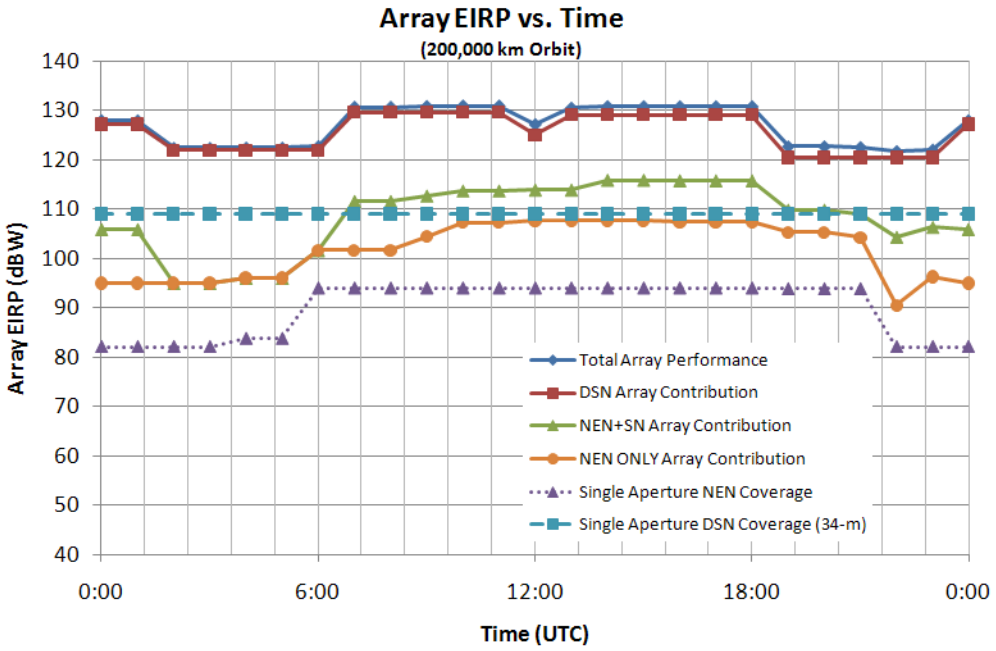

Figure 8.—SCaN Integrated Network Array EIRP performance for a 200,000 km orbit over a 24-hr period.

The key conclusions to be drawn from this analysis are as follows:

1. Total SCaN Integrated Network Array EIRP performance is dominated by the DSN array EIRP, as these elements possess the highest gain and transmitter power/element. However, the contribution of NEN and SN arraying is apparent, though marginalized to less than 2 dB for extra-lunar orbits.
2. Within a given network (i.e., the DSN array, NEN array, or the combined NEN+SN array), array EIRP performance is significantly enhanced over the state-of-practice use of a single antenna element.
   - Arraying of all Canberra DSN assets (two 34-m and one 70-m antenna) indicates an approximate 10-dB improvement in EIRP relative to a single 34-m DSN antenna (dashed blue line), and a 5-dB improvement in EIRP relative to a single 70-m DSN antenna (not shown in figure).
   - For periods of time when multiple DSN sites are in view of a spacecraft (i.e., Canberra and Goldstone), DSN arraying improves EIRP by more than 20 dB relative to a single 34-m DSN antenna, or a 15-dB improvement relative to a single 70-m DSN antenna.
   - NEN arraying (solid orange line) can provide 20 to 30 dB improvement in EIRP over the state-of-practice implementation of a single 13-m aperture antenna with 500W transmitter power (dotted purple line).
   - For an integrated NEN+SN ground station array (solid green line), an additional 6 to 8 dB improvement in EIRP over solely NEN arraying is realizable for most orbital arrangements.
3. Over the course of a 24-hr period for an equatorial sub-lunar orbit (200,000 km), network-centric arraying provides 10 to 15 dB improvement in EIRP link margin.

3.0 Conclusions

Utilizing arraying technology for the future SCaN Integrated Network architecture represents an optimal realization of NASA communications resources. However, several implementation and return on investment issues arise when considering the development of a fully integrated SCaN Network Array:

- Implementation of a SCaN Integrated Network Array will require spectrum sharing, or some form of adaptable common spectrum use, to realize cross-network arraying. This implementation is currently not being considered in the development of the next generation SCaN Integrated Network and would require some modification to the current development plan.
- More importantly, arraying the DSN element with either of the NEN or SN elements provides no improvement in receive array performance and only marginal improvements (< 2 dB excess margin) in transmit array performance. ***Therefore, implementation of this approach should not be furthered.***

Based on these results, it is determined that the best way to proceed in implementing an arraying technology development plan and architecture is to focus on network-centric arraying. This implementation plan would provide the most straightforward and optimal return on investment strategy for realizing receive/transmit arraying for the NASA's communications infrastructure.

- A network-centric implementation will be straightforward since arraying technology is already being developed along this path within the various networks. Further, common spectrum use required for coherent arraying are already resolved within individual networks.
- Network-centric arraying can provide substantial improvement in receive and transmit arraying relative to the current state of practice of single aperture implementation. The return on investment under this approach is significantly greater than implementing a fully integrated SCaN network array.

Appendix A.—Derivation of Array G/T

Let us consider an array of N antennas, each characterized by a gain, G_i, and a system temperature, T_i. Let us further assume that the phasing amongst antenna elements are perfectly matched to maximize the signal to noise ratio (SNR) of the receive arrayed signal in the direction of the incident narrowband signal via appropriate phase compensation and weighting and that the arraying is performed at some baseband frequency, f. For the given antenna assets in view of a particular spacecraft at some time, t, the summed voltage signal at baseband can therefore be described by,

$$v_{array}(f,t) = \sum_{i=1}^{N} \alpha_i e^{-j\phi_i} v_i(f, t+\tau_i) \tag{A.1}$$

where N is the number of arrayed antennas in view of the spacecraft, vi is the baseband voltage at the receiver, τ_i is the geometrical phase delay of the array elements in the direction of propagation, and $\alpha_i e^{-j\phi i}$ is the complex amplitude and phase weighting factor applied to each individual antenna. From the definition of power, the arrayed receive power is related to the summed array voltages by,

$$P_{array} = \langle \int_0^{\Delta f} \left| v_{array}(f,t) \right|^2 df \rangle \tag{A.2a}$$

$$= \langle \int_0^{\Delta f} \left[v_{array}(f,t) \right] \left[v^*_{array}(f,t) \right] df \rangle \tag{A.2b}$$

$$= \langle \int_0^{\Delta f} \left[\sum_{i=1}^{N} \alpha_i e^{-j\phi_i} v_i(f, t+\tau_i) \right] \left[\sum_{k=1}^{N} \alpha_k e^{j\phi_k} v^*_k(f, t+\tau_k) \right] df \rangle \tag{A.2c}$$

$$= \langle \int_0^{\Delta f} \left[\sum_{i=1}^{N} \alpha_i^2 |v_i(f, t+\tau_i)|^2 + \sum_{i=1}^{N} \sum_{\substack{k=1 \\ i \neq k}}^{N} \alpha_i \alpha_k e^{-j\phi_i + j\phi_k} v_i(f, t+\tau_i) v^*_k(f, t+\tau_k) \right] df \rangle \tag{A.2d}$$

$$= \sum_{i=1}^{N} \alpha_i^2 P_i + \sum_{i=1}^{N} \sum_{\substack{k=1 \\ i \neq k}}^{N} \alpha_i \alpha_k \rho_{ik} \tag{A.2e}$$

where <…> denotes the time average, and P_i is the single dish power from the i^{th} antenna given by,

$$P_i = \langle \int_0^{\Delta f} df |v_i(f, t+\tau_i)|^2 \rangle \tag{A.3}$$

and ρ_{ik} is the unnormalized correlation between the i^{th} and k^{th} antennas described by,

$$\rho_{ik} = \langle \int_0^{\Delta f} e^{-j\phi_i + j\phi_k} v_i(f, t+\tau_i) v^*_k(f, t+\tau_k) df \rangle \tag{A.4}$$

Since the arrayed power consists of an arrayed signal power and an arrayed noise power, we can derive the following expressions for each based on the above equations.

$$P_{array}^{signal} = \sum_{i=1}^{N} \alpha_i^2 P_i^{signal} + \sum_{i=1}^{N} \sum_{\substack{k=1 \\ i \neq k}}^{N} \alpha_i \alpha_k \rho_{ik}^{signal} \tag{A.5}$$

$$P_{array}^{noise} = \sum_{i=1}^{N} \alpha_i^2 P_i^{noise} + \sum_{i=1}^{N} \sum_{\substack{k=1 \\ i \neq k}}^{N} \alpha_i \alpha_k \rho_{ik}^{noise} \tag{A.6}$$

$$P_{array}^{noise} \approx \sum_{i=1}^{N} \alpha_i^2 P_i^{noise} \tag{A.7}$$

where we have noted that the arrayed noise power is accurately approximated by the sum of the weighted individual element noise powers, due to the fact that uncorrelated noise will be present in each signal path due to the large separation distance of each antenna element.

Therefore, the output array G/T can be related to the array output SNR by,

$$\left.\frac{G}{T}\right|_{array} \propto \frac{P_{array}^{signal}}{P_{array}^{noise}} = \frac{\sum_{i=1}^{N} \alpha_i^2 P_i^{signal} + \sum_{i=1}^{N} \sum_{\substack{k=1 \\ i \neq k}}^{N} \alpha_i \alpha_k \rho_{ik}^{signal}}{\sum_{i=1}^{N} \alpha_i^2 P_i^{noise}} \tag{A.8}$$

To determine a final expression for array G/T, we can relate the receive signal power, the cross-correlated signal power component, and the noise power to the antenna gain and system temperatures (ignoring any path loss contributions and assuming maximal phasing conditions) by,

$$P_i^{signal} \equiv P^{tx} G_i \tag{A.9}$$

$$\rho_{ik}^{signal} \equiv \sqrt{P^{tx} G_i} \sqrt{P^{tx} G_k} = P^{tx} \sqrt{G_i G_k} \tag{A.10}$$

$$P_i^{noise} \equiv k_B T_i \Delta f \tag{A.11}$$

where k_B is Boltzmann's constant, P^{tx} is the transmit power from, i.e., the spacecraft, G_i is the individual antenna system gain, T_i is the individual antenna system temperature, and Δf is the bandwidth at the output of the beamformer. Thus, the G/T for an array as a function of individual antenna element gain and system temperature is,

$$\frac{G}{T}_{array} = \frac{\sum_{i=1}^{N} \alpha_i^2 G_i + \sum_{i=1}^{N} \sum_{\substack{k=1 \\ i \neq k}}^{N} \alpha_i \alpha_k \sqrt{G_i G_k}}{\sum_{i=1}^{N} \alpha_i^2 T_i + T_{B\_eff}} = \frac{\left(\sum_{i=1}^{N} \alpha_i \sqrt{G_i}\right)^2}{\sum_{i=1}^{N} \alpha_i^2 T_i + T_{B\_eff}} \tag{A.12}$$

where the term, T_{B_eff} has been introduced to account for the correlated system noise temperature potentially "seen" in common by the antenna elements, as contributed by the atmospheric brightness temperature. For the case of completely uncorrelated noise contributions (very far apart antenna elements), let us presume that the effective brightness temperature contribution is minimal. Thus, to ensure optimal combining of the receive signal, the weighting factors, α_i, should be chosen so as to maximize the array G/T. Such α_i will satisfy the equation:

$$\frac{d(G/T)}{d\alpha_j} = 0 \tag{A.13}$$

$$\frac{d(G/T)}{d\alpha_j} = \frac{2\alpha_j G_j + 2\sum_{\substack{k=1 \\ k\neq j}}^{N} \alpha_k \sqrt{G_j G_k}}{\sum_{i=1}^{N} \alpha_i^2 T_i} - \frac{2\alpha_j T_j \left(\sum_{i=1}^{N} \alpha_i^2 G_i + \sum_{i=1}^{N} \sum_{\substack{k=1 \\ i\neq k}}^{N} \alpha_i \alpha_k \sqrt{G_i G_k} \right)}{\left(\sum_{i=1}^{N} \alpha_i^2 T_i \right)^2} \tag{A.14}$$

$$= \frac{\left(\sum_{i=1}^{N} \alpha_i^2 T_i \right) \left(2\alpha_j G_j + 2\sum_{\substack{k=1 \\ k\neq j}}^{N} \alpha_k \sqrt{G_j G_k} \right) - 2\alpha_j T_j \left(\sum_{i=1}^{N} \alpha_i^2 G_i + \sum_{i=1}^{N} \sum_{\substack{k=1 \\ i\neq k}}^{N} \alpha_i \alpha_k \sqrt{G_i G_k} \right)}{\left(\sum_{i=1}^{N} \alpha_i^2 T_i \right)^2} \tag{A.15}$$

The above equation will equal zero when the numerator is equal to zero. Thus,

$$0 = \sum_{i=1}^{N} \alpha_i^2 T_i \left(2\alpha_j G_j + 2\sum_{\substack{k=1 \\ k\neq j}}^{N} \alpha_k \sqrt{G_j G_k} \right) - 2\alpha_j T_j \left(\sum_{i=1}^{N} \alpha_i^2 G_i + \sum_{i=1}^{N} \sum_{\substack{k=1 \\ i\neq k}}^{N} \alpha_i \alpha_k \sqrt{G_i G_k} \right) \tag{A.16}$$

Solving the *N* equations for *N* unknowns, it can be shown that the optimal weights for maximum array G/T is determined to be,

$$\alpha_i = \frac{\sqrt{G_i}}{T_i} \tag{A.17}$$

Note that in the case of correlated atmospheric brightness temperature contribution (i.e., for the case of antenna elements located in approximately the same geophysical location), the optimal weight calculation will be biased by some amount. However, it has been shown that this contribution produces an error of approximately 10% in the optimal weight determination which can be considered negligible for the purposes of this analysis.[3]

[3]R. Dewey, "The Effects of Correlated Noise in Intra-Complex DSN Arrays for S-Band Galileo Telemetry Reception," TDA Progress Report 42-111, November 15, 1992.

Appendix B.—Derivation of Array EIRP

From the transmitted power perspective, in the optimal case, we know that for a widely distributed array, the maximum achievable arraying gain, G_{array}, is given simply by the sum of the individual antenna gains, G_n.

$$\vec{E}_{array}(r,\theta,\phi) = \left(\frac{e^{-jkR}}{2\pi R}\right)\sum_{m=1}^{N}\left(C_m e^{j\varphi_m}\right) f_m(\theta,\phi) e^{-jk\hat{a}_r\cdot\vec{\rho}_m} \tag{B.1}$$

where, k is the wavenumber ($2\pi/\lambda$), $f_m(\theta,\phi)$ is the individual antenna voltage pattern,

The array radiation intensity is described by,

$$U(\theta,\phi) = \frac{r^2}{2\eta}\left|\vec{E}_{array}(r,\theta,\phi)\right|^2 \tag{B.2}$$

$$= \frac{k^2}{8\pi^2\eta}\sum_{m=1}^{N}\sum_{n=1}^{N} f_m(\theta,\phi) f_n(\theta,\phi)^* e^{j(\varphi_m-\varphi_n)} \tag{B.3}$$

The total radiated power for an array with elements spaced vary far apart ($d >> \lambda$) is approximated by

$$P_{rad} = \int_0^{2\pi}\int_0^{\pi/2} U(\theta,\phi)\sin\theta\, d\theta d\phi \tag{B.4}$$

$$= \frac{\pi k^2}{\eta}\int_0^{\pi/2}\left(\sum_{m=1}^{N}|f_m(\theta,\phi)|^2\right) sin\,\theta\, d\theta \tag{B.5}$$

If, for analytical simplicity, we assume that no blockage occurs and that the reflectors are uniformly illuminated by a linearly polarized feed, and the inter-element phasing is such that the peak of the array pattern is directed to zenith, the antenna element field pattern of a circular aperture can be described by,

$$f_m(\theta,\phi) = jk\varepsilon_m\left[2\pi a_m^2\frac{J_1(ka_m\sin\theta)}{ka_m\sin\theta}\right] \tag{B.6}$$

where a_m is the reflector antenna diameter, ε_m is the individual antenna efficiency, and J_1 is the Bessel function of first order. From this assumption, the array gain can readily be determined as,

$$U_0 \equiv U(\theta=0) = \frac{k^2}{8\eta}\sum_{m=1}^{N}\sum_{n=1}^{N} a_m^2 a_n^2 \tag{B.7}$$

$$P_{rad} = \frac{\pi}{2\eta}\sum_{m=1}^{N} a_m^2 \tag{B.8}$$

$$G_{array} = \frac{4\pi U_0}{P_{rad}} = \frac{4\pi^2}{\lambda^2}\sum_{n=1}^{N} a_n^2 = \sum_{n=1}^{N} G_n \tag{B.9}$$

where it is observed that the total array gain simplifies to the sum of the individual antenna element gains for a widely distributed array. This solution is valid for any arbitrary array in which the separation distance between elements is much greater than the wavelength of operation.

The total transmit power is given simply by the sum of the individual element transmit powers (P_m). Therefore the optimally combined array EIRP is easily defined as:

$$EIRP_{array} = G_{array} \sum_{m=1}^{N} P_m = \left[\sum_{n=1}^{N} G_n\right]\left[\sum_{m=1}^{N} P_m\right] \tag{B.10}$$

Note that for an array of identical antenna elements with equal transmit powers, we obtain the well-known improvement in array EIRP as N^2 times the individual antenna element EIRP. However, for an array of dissimilar antenna elements, this maximal improvement is weighted by the relative levels of each individual element, as will be shown in the results of the integrated network array.

Appendix C.—State-of-Practice DSN Antenna Specifications[4]

	Antenna Asset (ID)	Antenna Diameter	Location (km) x	Location (km) y	Location (km) z	Frequency Use	Aperture Gain (dB)	Noise Temperature (K)	G/T (dB/K)	Transmitter Power (dBW)	Transmitter Gain (dBi)	EIRP (dBW)
Goldstone DSN	DSS-14	70-m	-2353.62	-4641.34	3677.05	S-band Transmit Frequencies (2110 to 2120 MHz)	61.6			42.65	62.95	105.6
						X-band Transmit Frequencies (7145 to 7190 MHz)	72.2			42.57	73.23	115.8
						L-Band Receive Frequencies (1628 to 1708 MHz)	59.5	26.68	61.04			
						S-Band Receive Frequencies (2270 to 2300 MHz)	62.3	15.00	63.59			
						X-Band Receive Frequencies (8400 to 8500 MHz)	73.6	11.65	74.55			
	DSS-15	34-m	-2353.54	-4641.65	3676.67	X-Band Transmit Frequencies (7145 to 7190 MHz)	65.9			42.75	67.05	109.8
						S-Band Receive Frequencies (2200–2300 MHz)	55.9	34.00	56.07			
						X-Band Receive Frequencies (8400–8500 MHz)	67.3	32.37	68.41			
	DSS-24	34-m	-2354.91	-4646.84	3669.24	S-Band Transmit Frequencies (2025–2120 MHz)	55.1			42.4	56.25	98.65
						X-Band Transmit Frequencies (7145–7235 MHz)	65.9			41.8	67.9	109.7
						S-Band Receive Frequencies (2200–2300 MHz)	55.9	26.50	41.62			
						K-Band Receive Frequencies (25500–27000 MHz)	77.2	20.70	64.03			
						X-Band Receive Frequencies (8400–8500 MHz)	67.3	21.28	54.07			
	DSS-25	34-m	-2355.02	-4646.95	3669.04	X-Band Transmit Frequencies (7145–7235 MHz)	65.9			42.6	67.1	109.7
						Ka-Band Transmit Frequencies (34200.34700 MHz)	79.6			28.72	79.5	108.22
						X-Band Receive Frequencies (8400–8500 MHz)	67.3	20.20	54.30			
						Ka-Band Receive Frequencies (31800–32300 MHz)	78.9	27.89	64.47			
	DSS-26	34-m	-2354.89	-4647.17	3668.87	X-Band Transmit Frequencies (7145–7235 MHz)	65.9			39.4	67.1	106.5
						X-Band Receive Frequencies (8400–8500 MHz)	67.3	15.43	55.47			
						Ka-Band Receive Frequencies (31800–32300 MHz)	78.9	19.36	66.06			
	DSS-27	34-m	-2349.92	-4656.76	3660.1	S-Band Transmit Frequencies (2025–2120 MHz)	55.1			22.4	54.34	76.74
						S-Band Receive Frequencies (2200–2300 MHz)	55.9	102.00	35.77			
Canberra DSN	DSS-34	34-m	-4504.61	2708.57	-3601.96	S-Band Transmit Frequencies (2025–2120 MHz)	55.1			42.4	56.25	98.65
						X-Band Transmit Frequencies (7145–7235 MHz)	65.9			39.41	67.09	106.5
						S-Band Receive Frequencies (2200–2300 MHz)	55.9	18.00	43.30			
						X-Band Receive Frequencies (8400–8500 MHz)	67.3	16.28	55.23			
						K-Band Receive Frequencies (25500–27000 MHz)	77.2	25.60	63.11			
						Ka-Band Receive Frequencies (31800–32300 MHz)	78.9	19.38	66.05			
	DSS-43	70-m	-4504.79	2708.76	-3601.6	S-Band Transmit Frequencies (2010 to 2120 MHz)	61.4			45.1	62.95	108.05
						X-band Transmit Frequencies (7145 to 7190 MHz)	72.2			42.57	73.23	115.8
						L-Band Receive Frequencies (1628 to 1708 MHz)	59.5	26.68	45.27			
						S-Band Receive Frequencies (2270 to 2300 MHz)	62.3	16.00	50.22			
						X-Band Receive Frequencies (8400 to 8500 MHz)	73.6	12.10	62.79			
	DSS-45	34-m	-4504.4	2708.9	-3601.95	S-Band Transmit Frequencies (2025 to 2110 MHz)	55.1			23.4	55.4	78.8
						X-Band Transmit Frequencies (7145 to 7190 MHz)	65.9			42.75	67.05	109.8
						S-Band Receive Frequencies (2200–2300 MHz)	55.9	41.76	39.65			
						X-Band Receive Frequencies (8400–8500 MHz)	67.3	32.37	52.25			
Madrid DSN	DSS-54	34-m	4849.42	-360.723	4114.61	S-Band Transmit Frequencies (2025–2122 MHz)	55.1			42.4	56.25	98.65
						X-Band Transmit Frequencies (7147–7235 MHz)	65.9			39.41	67.09	106.5
						S-Band Receiver Frequency 2200–2300 MHz	55.9	20.03	42.84			
						X-Band Receiver Frequency 8400–8500 MHz	67.3	18.31	54.72			
						K-Band Receiver Frequency 25500–27000 MHz	77.2	28.80	62.60			
						Ka-Band Receiver Frequency 31800–32300 MHz	78.9	21.80	65.54			
	DSS-55	34-m	4849.51	-360.605	4114.48	S-Band Transmit Frequencies (2025–2122 MHz)	55.1			42.4	56.25	98.65
						X-Band Transmit Frequencies (7147–7235 MHz)	65.9			39.4	67.1	106.5
						S-Band Receiver Frequency 2200–2300 MHz	55.9	20.03	42.84			
						X-Band Receiver Frequency 8400–8500 MHz	67.3	17.42	54.94			
						Ka-Band Receiver Frequency 31800–32300 MHz	78.9	20.80	65.75			
	DSS-63	70-m	4849.07	-360.179	4115.09	S-Band Transmit Frequencies (2110 to 2120 MHz)	61.6			38.55	62.95	101.5
						X-band Transmit Frequencies (7145 to 7190 MHz)	72.2			42.57	73.23	115.8
						L-Band Receive Frequencies (1628 to 1708 MHz)	59.5	26.68	45.27			
						S-Band Receive Frequencies (2270 to 2300 MHz)	62.1	21.00	48.91			
						X-Band Receive Frequencies (8400 to 8500 MHz)	73.6	11.46	63.03			
	DSS-65	34-m	4849.33	-360.488	4114.74	S-Band Transmit Frequencies (2025 to 2110 MHz)	55.1			23.4	55.4	78.8
						X-Band Transmit Frequencies (7145 to 7190 MHz)	65.9			42.75	67.05	109.8
						S-Band Receive Frequencies (2200–2300 MHz)	55.9	41.76	39.65			
						X-Band Receive Frequencies (8400–8500 MHz)	67.3	32.37	52.25			

[4] JPL 810-005 Handbook

Appendix D.—State-of-Practice NEN Antenna Specifications[5]

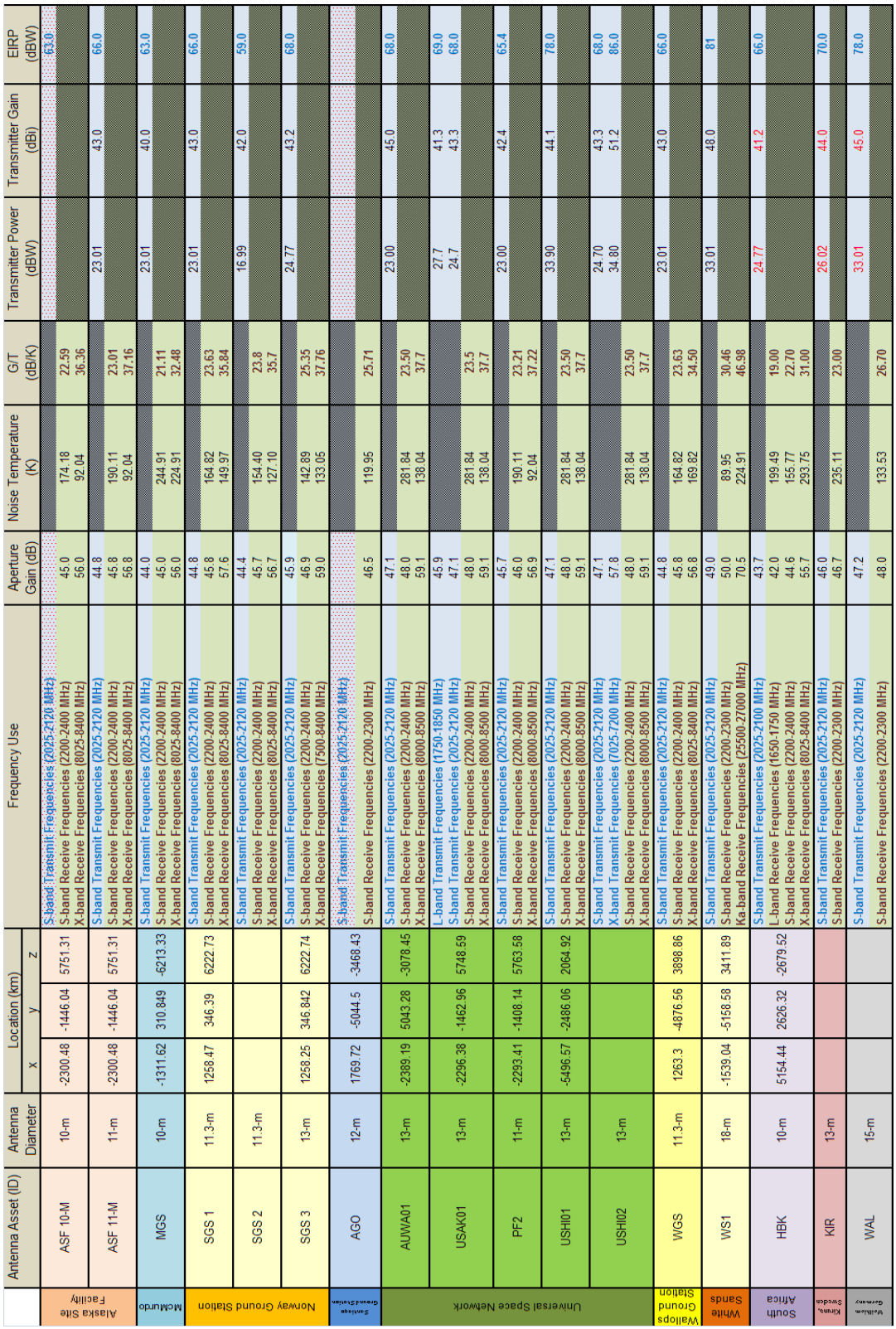

Antenna Asset (ID)		Antenna Diameter	Location (km)			Frequency Use	Aperture Gain (dB)	Noise Temperature (K)	G/T (dB/K)	Transmitter Power (dBW)	Transmitter Gain (dBi)	EIRP (dBW)
			x	y	z							
Alaska Site Facility	ASF 10-M	10-m	-2300.48	-1446.04	5751.31	S-band Transmit Frequencies (2025-2120 MHz)	45.0	174.18	22.59	23.01	43.0	66.0
						S-band Receive Frequencies (2200-2400 MHz)	56.0	92.04	36.36			
						X-band Receive Frequencies (8025-8400 MHz)						
	ASF 11-M	11-m	-2300.48	-1446.04	5751.31	S-band Transmit Frequencies (2025-2120 MHz)	44.8	190.11	23.01	23.01	43.0	66.0
						S-band Receive Frequencies (2200-2400 MHz)	45.8	92.04	37.16			
						X-band Receive Frequencies (8025-8400 MHz)	56.8					
McMurdo	MGS	10-m	-1311.62	310.849	-6213.33	S-band Transmit Frequencies (2025-2120 MHz)	44.0	244.91	21.11	23.01	40.0	63.0
						S-band Receive Frequencies (2200-2400 MHz)	45.0	224.91	32.48			
						X-band Receive Frequencies (8025-8400 MHz)	56.0					
Norway Ground Station	SGS 1	11.3-m	1258.47	346.39	6222.73	S-band Transmit Frequencies (2025-2120 MHz)	44.8	164.82	23.63	23.01	43.0	66.0
						S-band Receive Frequencies (2200-2400 MHz)	45.8	149.97	35.84			
						X-band Receive Frequencies (8025-8400 MHz)	57.6					
	SGS 2	11.3-m				S-band Transmit Frequencies (2025-2120 MHz)	44.4	154.40	23.8	16.99	42.0	59.0
						S-band Receive Frequencies (2200-2400 MHz)	45.7	127.10	35.7			
						X-band Receive Frequencies (8025-8400 MHz)	56.7					
	SGS 3	13-m	1258.25	346.842	6222.74	S-band Transmit Frequencies (2025-2120 MHz)	45.9	142.89	25.35	24.77	43.2	68.0
						S-band Receive Frequencies (2200-2400 MHz)	46.9	133.05	37.76			
						X-band Receive Frequencies (7500-8400 MHz)	59.0					
Santiago Ground Station	AGO	12-m	1769.72	-5044.5	-3468.43	S-band Transmit Frequencies (2025-2120 MHz)						
						S-band Receive Frequencies (2200-2300 MHz)	46.5	119.95	25.71	23.00	45.0	68.0
Universal Space Network	AUWA01	13-m	-2389.19	5043.28	-3078.45	S-band Transmit Frequencies (2025-2120 MHz)	47.1	281.84	23.50			
						S-band Receive Frequencies (2200-2400 MHz)	48.0	138.04	37.7			
						X-band Receive Frequencies (8000-8500 MHz)	59.1					
	USAK01	13-m	-2296.38	-1462.96	5748.59	L-band Transmit Frequencies (1750-1850 MHz)	45.9			27.7	41.3	69.0
						S-band Transmit Frequencies (2025-2120 MHz)	47.1			24.7	43.3	68.0
						S-band Receive Frequencies (2200-2400 MHz)	48.0	281.84	23.5			
						X-band Receive Frequencies (8000-8500 MHz)	59.1	138.04	37.7			
	PF2	11-m	-2293.41	-1408.14	5763.58	S-band Transmit Frequencies (2025-2120 MHz)	45.7			23.00	42.4	65.4
						S-band Receive Frequencies (2200-2400 MHz)	46.0	190.11	23.21			
						X-band Receive Frequencies (8000-8500 MHz)	56.9	92.04	37.22			
	USHI01	13-m	-5496.57	-2486.06	2064.92	S-band Transmit Frequencies (2025-2120 MHz)	47.1			33.90	44.1	78.0
						S-band Receive Frequencies (2200-2400 MHz)	48.0	281.84	23.50			
						X-band Receive Frequencies (8000-8500 MHz)	59.1	138.04	37.7			
	USHI02	13-m				S-band Transmit Frequencies (2025-2120 MHz)	47.1			24.70	43.3	68.0
						X-band Transmit Frequencies (7025-7200 MHz)	57.8			34.80	51.2	86.0
						S-band Receive Frequencies (2200-2400 MHz)	48.0	281.84	23.50			
						X-band Receive Frequencies (8000-8500 MHz)	59.1	138.04	37.7			
Wallops Ground Station	WGS	11.3-m	1263.3	-4876.56	3898.86	S-band Transmit Frequencies (2025-2120 MHz)	44.8			23.01	43.0	66.0
						S-band Receive Frequencies (2200-2400 MHz)	45.8	164.82	23.63			
						X-band Receive Frequencies (8025-8400 MHz)	56.8	169.82	34.50			
White Sands	WS1	18-m	-1539.04	-5158.58	3411.89	S-band Transmit Frequencies (2025-2120 MHz)	49.0			33.01	48.0	81
						S-band Receive Frequencies (2200-2300 MHz)	50.0	89.95	30.46			
						Ka-band Receive Frequencies (25500-27000 MHz)	70.5	224.91	46.98			
South Africa	HBK	10-m	5154.44	2626.32	-2679.52	S-band Transmit Frequencies (2025-2100 MHz)	43.7			24.77	41.2	66.0
						L-band Receive Frequencies (1650-1750 MHz)	42.0	199.49	19.00			
						S-band Receive Frequencies (2200-2400 MHz)	44.6	155.77	22.70			
						X-band Receive Frequencies (8025-8400 MHz)	55.7	293.75	31.00			
Kiruna, Sweden	KIR	13-m				S-band Transmit Frequencies (2025-2120 MHz)	46.0			26.02	44.0	70.0
						S-band Receive Frequencies (2200-2300 MHz)	46.7	235.11	23.00			
Weilheim Germany	WAL	15-m				S-band Transmit Frequencies (2025-2120 MHz)	47.2			33.01	45.0	78.0
						S-band Receive Frequencies (2200-2300 MHz)	48.0	133.53	26.70			

[5]B. Golden, SCaN "As-Is" Architecture Description Document

Appendix E.—State-of-Practice SN Ground Segment Antenna Specifications[5]

	Antenna Asset (ID)	Antenna Diameter	Location (km)			Frequency Use	Aperture Gain (dB)	Noise Temperature (K)	G/T (dBi)	Transmitter Power (dBW)	Transmitter Gain (dBi)	EIRP (dBW)
			x	y	z							
Guam	SGL (GRGT)	16.5-m	-5069.92	3568.95	1491.61	Ku-band Transmit Frequencies (14.6-15.25GHz)	65.3			33.01029996	64.3	97.3
						Ku-band Receive Frequencies (13.4-14.05GHz)	64.5	220.00	41.05013582			
	SGLT-6 (GRGT)	11-m	-5069.92	3568.95	1491.61	Ku-band Transmit Frequencies (14.6-15.25GHz)	61.7			33.01029996	60.7	93.8
						Ku-band Receive Frequencies (13.4-14.05GHz)	61.0	220.00	37.52831064			
	SGLT-7 (GRGT)	16.5-m	-5069.92	3568.95	1491.61	Ku-band Transmit Frequencies (14.6-15.25GHz)	65.3			33.01029996	64.3	97.3
						Ku-band Receive Frequencies (13.4-14.05GHz)	64.5	220.00	41.05013582			
White Sands	SGLT-4 (WSGT)	18.3-m	-1538.98	-5158.45	3412.12	Ku-band Transmit Frequencies (14.6-15.25GHz)	66.2			33.01029996	65.2	98.2
						Ku-band Receive Frequencies (13.4-14.05GHz)	65.4	220.00	41.94947873			
	SGLT-5 (WSGT)	18.3-m	-1538.98	-5158.45	3412.12	Ku-band Transmit Frequencies (14.6-15.25GHz)	66.2			33.01029996	65.2	98.2
						Ku-band Receive Frequencies (13.4-14.05GHz)	65.4	220.00	41.94947873			
	SGLT-1 (STGT)	19-m	-1538.98	-5158.45	3412.12	Ku-band Transmit Frequencies (14.6-15.25GHz)	66.5			33.01029996	65.5	98.5
						Ku-band Receive Frequencies (13.4-14.05GHz)	65.7	220.00	42.27552896			
	SGLT-2 (STGT)	19-m	-1538.98	-5158.45	3412.12	Ku-band Transmit Frequencies (14.6-15.25GHz)	66.5			33.01029996	65.5	98.5
						Ku-band Receive Frequencies (13.4-14.05GHz)	65.7	220.00	42.27552896			
	SGLT-3 (STGT)	19-m	-1538.98	-5158.45	3412.12	Ku-band Transmit Frequencies (14.6-15.25GHz)	66.5			33.01029996	65.5	98.5
						Ku-band Receive Frequencies (13.4-14.05GHz)	65.7	220.00	42.27552896			

Appendix F.—Simulated Ground Segment Visibilities to Spacecraft (STK)

The following STK plots indicate ground station LOS availability for an equatorial orbiting spacecraft at various distances from Earth. The diagram below depicts how these plots are to be interpreted. The reader must refer back to Appendices C to E to identify the particular antenna assets being arrayed.

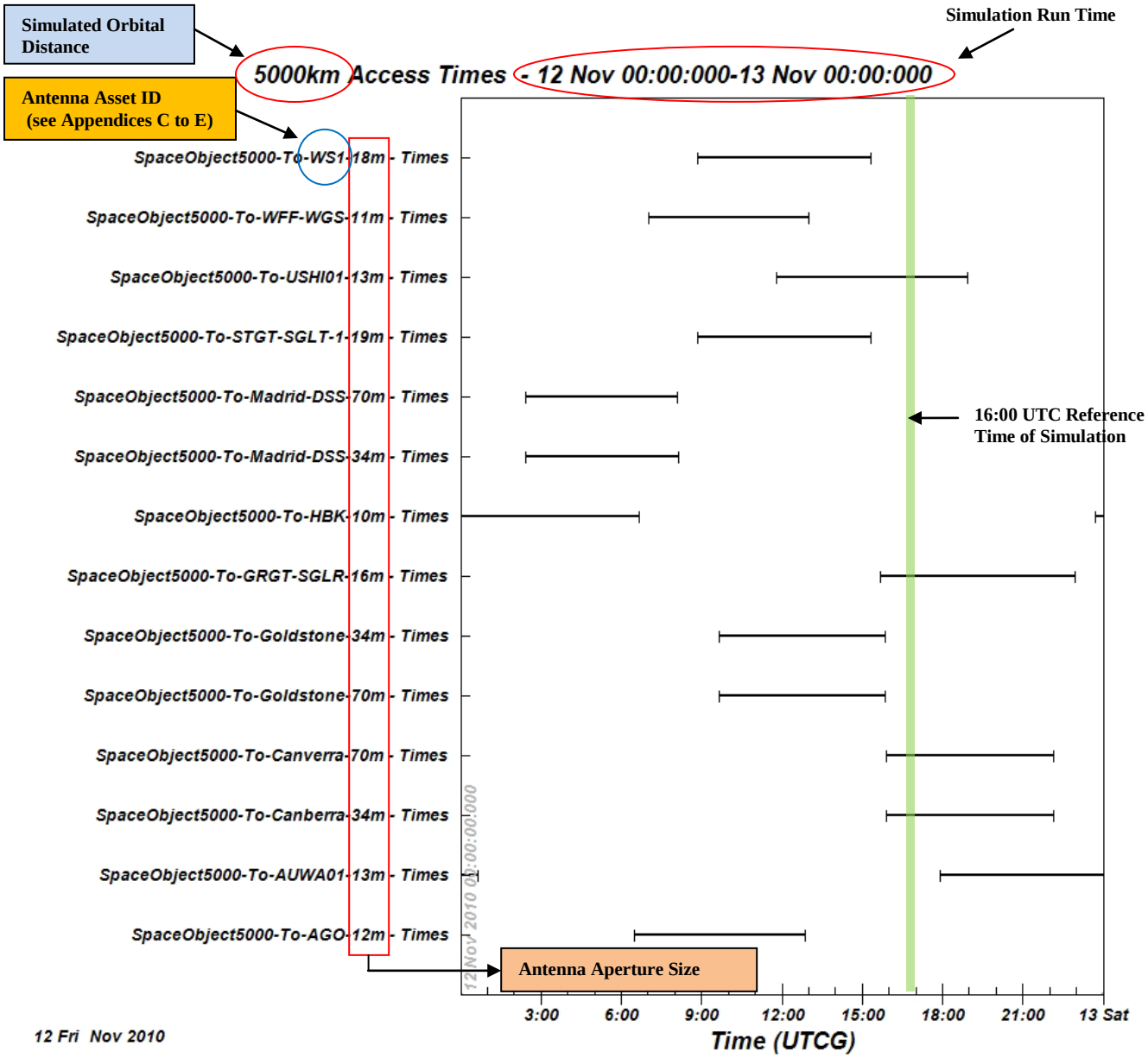

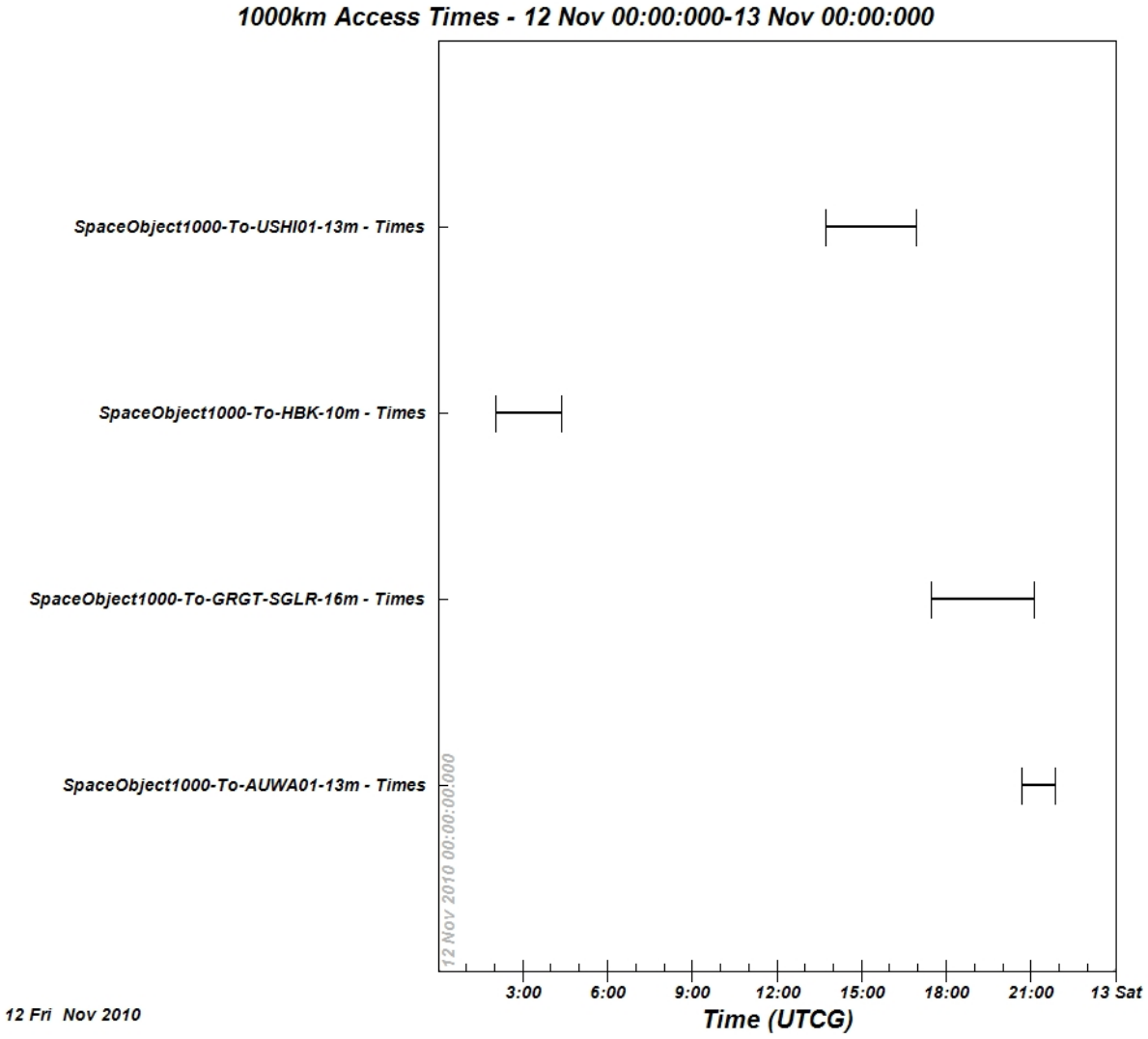
1000km Access Times - 12 Nov 00:00:000-13 Nov 00:00:000
SpaceObject1000-To-USHI01-13m - Times
SpaceObject1000-To-HBK-10m - Times
SpaceObject1000-To-GRGT-SGLR-16m - Times
SpaceObject1000-To-AUWA01-13m - Times
12 Nov 2010 00:00:00.000
3:00
6:00
9:00
12:00
15:00
18:00
21:00
13 Sat
12 Fri Nov 2010
Time (UTCG)

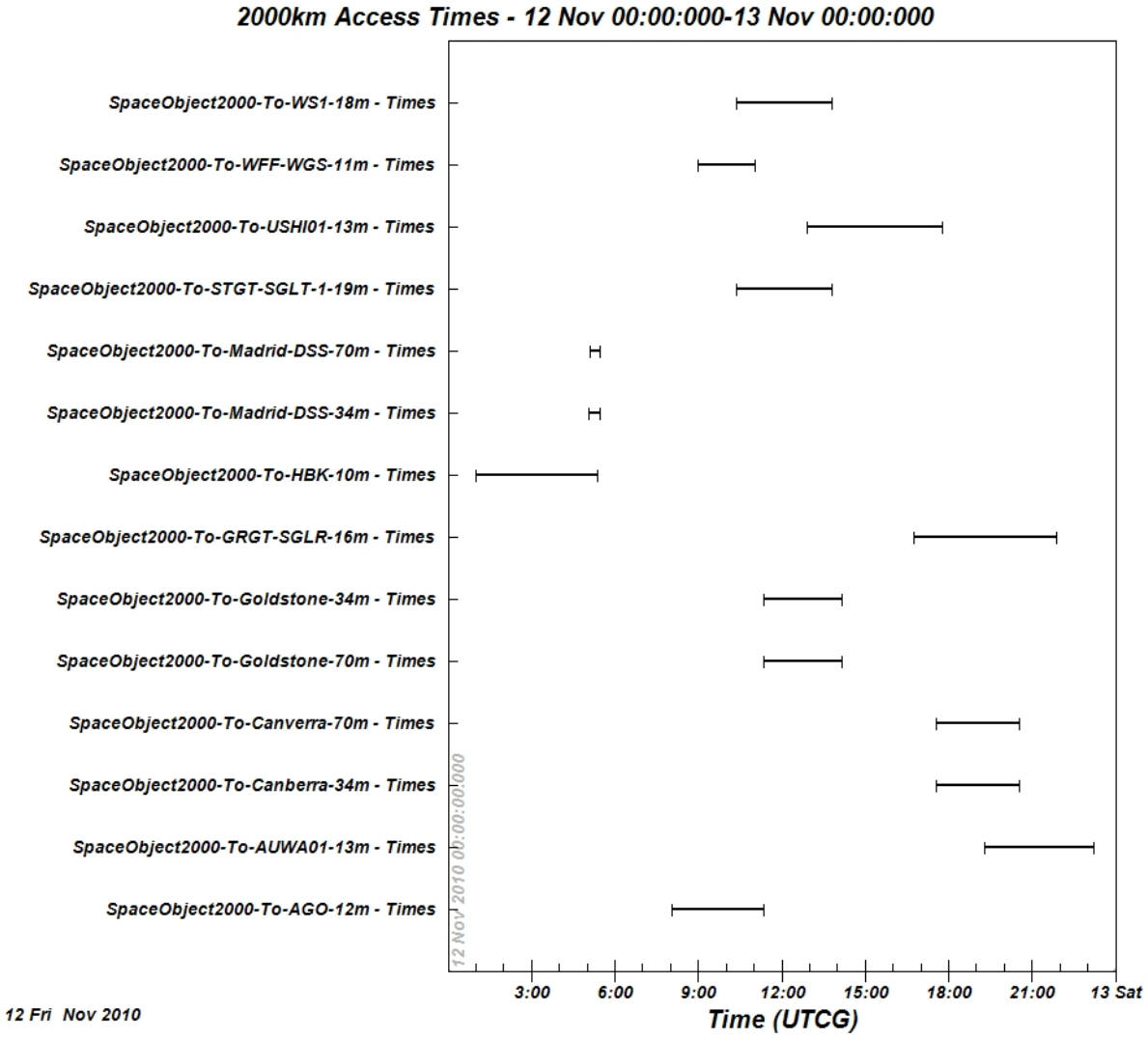
2000km Access Times - 12 Nov 00:00:000-13 Nov 00:00:000
SpaceObject2000-To-WS1-18m - Times
SpaceObject2000-To-WFF-WGS-11m - Times
SpaceObject2000-To-USHI01-13m - Times
SpaceObject2000-To-STGT-SGLT-1-19m - Times
SpaceObject2000-To-Madrid-DSS-70m - Times
SpaceObject2000-To-Madrid-DSS-34m - Times
SpaceObject2000-To-HBK-10m - Times
SpaceObject2000-To-GRGT-SGLR-16m - Times
SpaceObject2000-To-Goldstone-34m - Times
SpaceObject2000-To-Goldstone-70m - Times
SpaceObject2000-To-Canverra-70m - Times
SpaceObject2000-To-Canberra-34m - Times
SpaceObject2000-To-AUWA01-13m - Times
SpaceObject2000-To-AGO-12m - Times
12 Nov 2010 00:00:00.000
12 Fri Nov 2010
3:00
6:00
9:00
12:00
15:00
18:00
21:00
13 Sat
Time (UTCG)

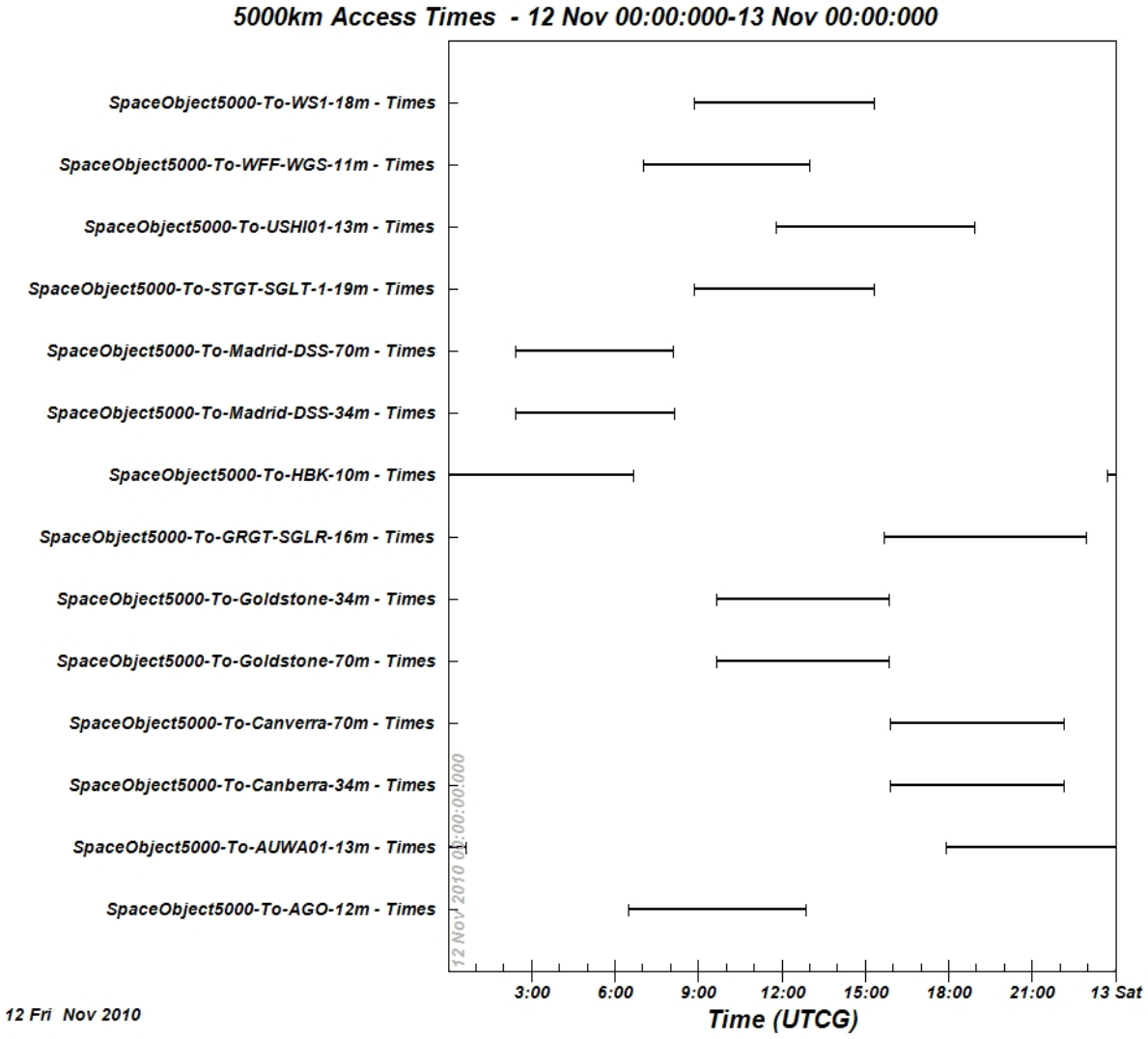
5000km Access Times - 12 Nov 00:00:000-13 Nov 00:00:000
SpaceObject5000-To-WS1-18m - Times
SpaceObject5000-To-WFF-WGS-11m - Times
SpaceObject5000-To-USHI01-13m - Times
SpaceObject5000-To-STGT-SGLT-1-19m - Times
SpaceObject5000-To-Madrid-DSS-70m - Times
SpaceObject5000-To-Madrid-DSS-34m - Times
SpaceObject5000-To-HBK-10m - Times
SpaceObject5000-To-GRGT-SGLR-16m - Times
SpaceObject5000-To-Goldstone-34m - Times
SpaceObject5000-To-Goldstone-70m - Times
SpaceObject5000-To-Canverra-70m - Times
SpaceObject5000-To-Canberra-34m - Times
SpaceObject5000-To-AUWA01-13m - Times
SpaceObject5000-To-AGO-12m - Times
12 Nov 2010 00:00:00.000
3:00
6:00
9:00
12:00
15:00
18:00
21:00
13 Sat
Time (UTCG)
12 Fri Nov 2010

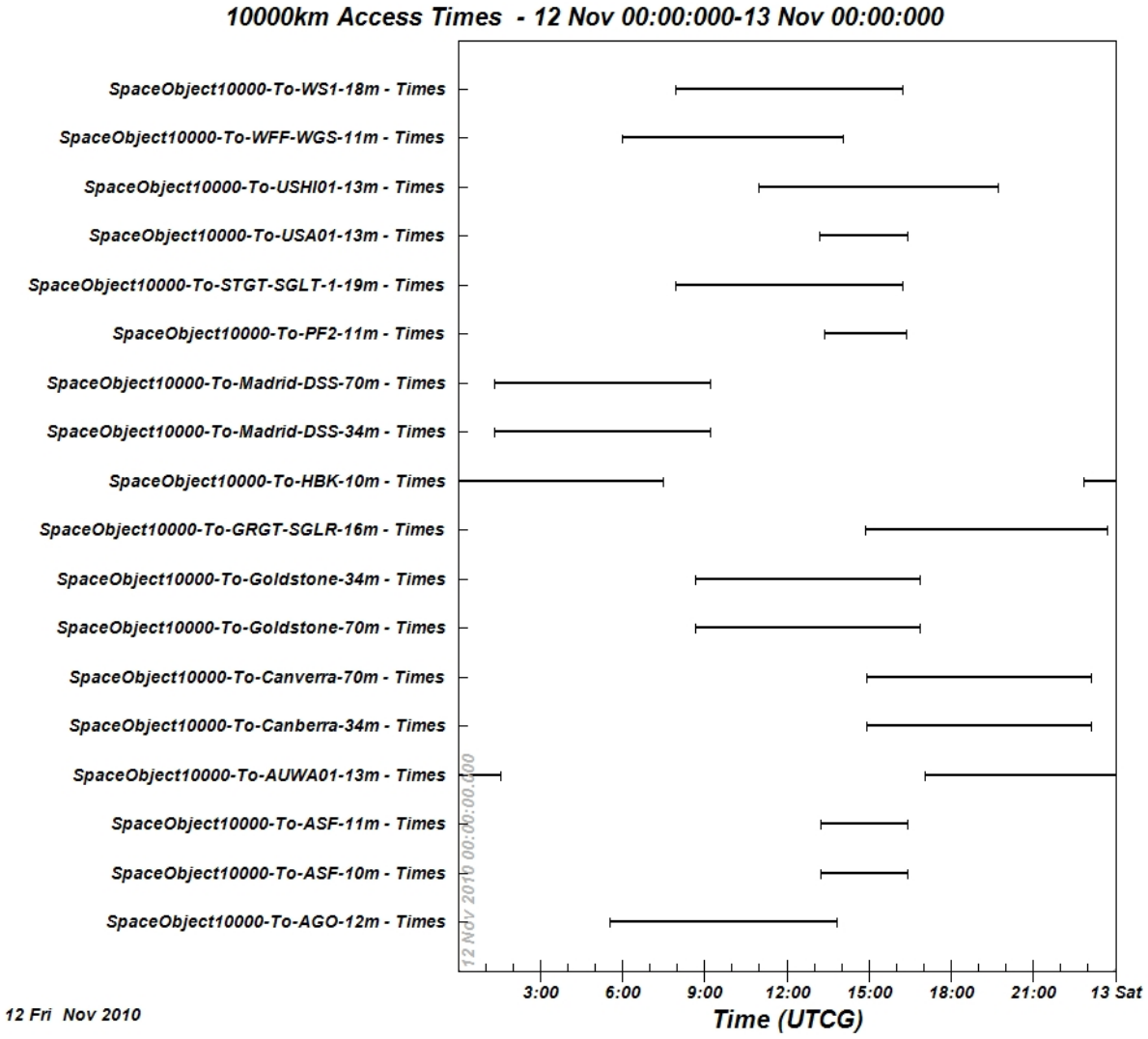
10000km Access Times - 12 Nov 00:00:000-13 Nov 00:00:000
SpaceObject10000-To-WS1-18m - Times
SpaceObject10000-To-WFF-WGS-11m - Times
SpaceObject10000-To-USHI01-13m - Times
SpaceObject10000-To-USA01-13m - Times
SpaceObject10000-To-STGT-SGLT-1-19m - Times
SpaceObject10000-To-PF2-11m - Times
SpaceObject10000-To-Madrid-DSS-70m - Times
SpaceObject10000-To-Madrid-DSS-34m - Times
SpaceObject10000-To-HBK-10m - Times
SpaceObject10000-To-GRGT-SGLR-16m - Times
SpaceObject10000-To-Goldstone-34m - Times
SpaceObject10000-To-Goldstone-70m - Times
SpaceObject10000-To-Canverra-70m - Times
SpaceObject10000-To-Canberra-34m - Times
SpaceObject10000-To-AUWA01-13m - Times
SpaceObject10000-To-ASF-11m - Times
SpaceObject10000-To-ASF-10m - Times
SpaceObject10000-To-AGO-12m - Times
12 Nov 2010 00:00:00.000
3:00
6:00
9:00
12:00
15:00
18:00
21:00
13 Sat
Time (UTCG)
12 Fri Nov 2010

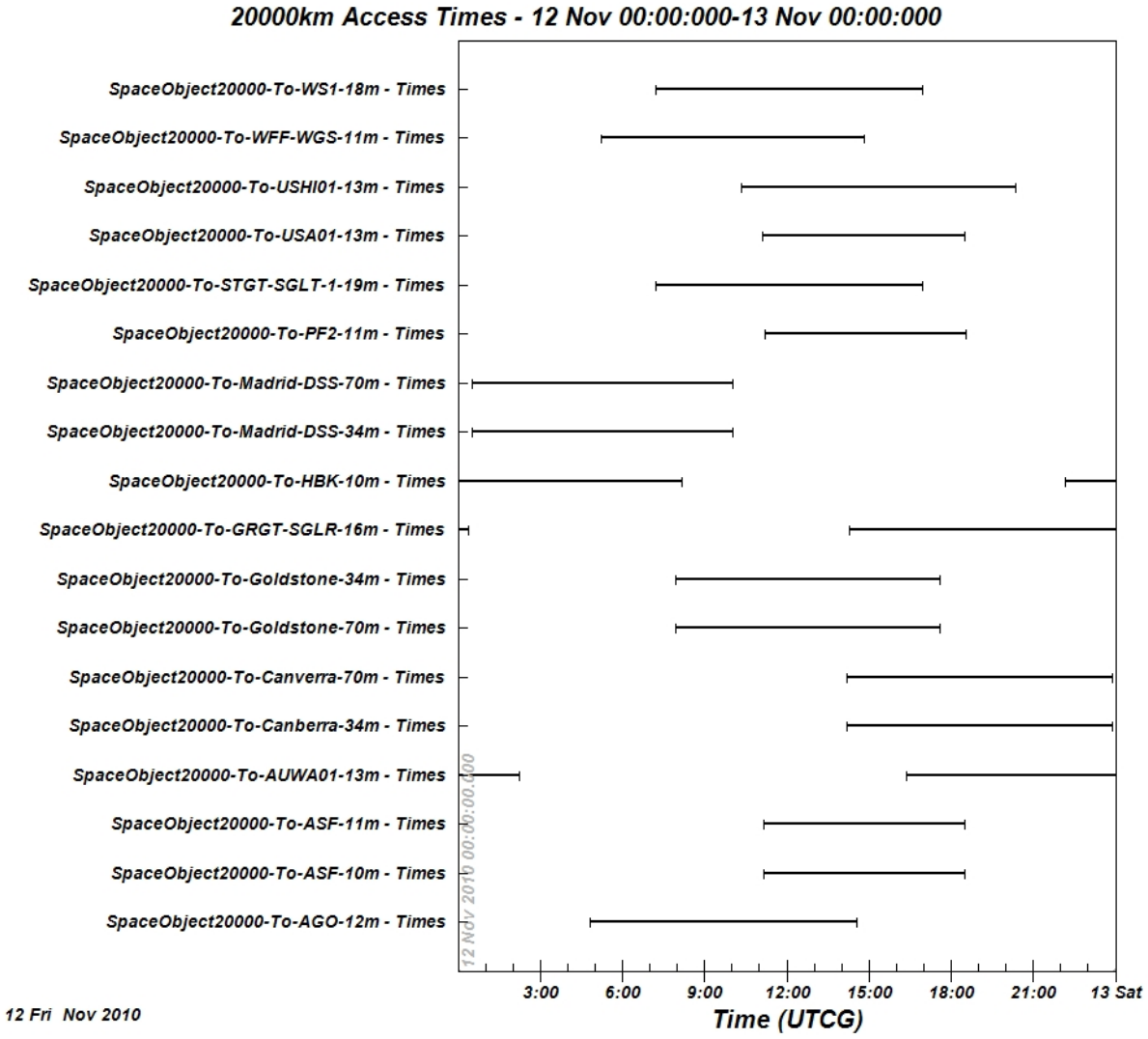
20000km Access Times - 12 Nov 00:00:000-13 Nov 00:00:000
SpaceObject20000-To-WS1-18m - Times
SpaceObject20000-To-WFF-WGS-11m - Times
SpaceObject20000-To-USHI01-13m - Times
SpaceObject20000-To-USA01-13m - Times
SpaceObject20000-To-STGT-SGLT-1-19m - Times
SpaceObject20000-To-PF2-11m - Times
SpaceObject20000-To-Madrid-DSS-70m - Times
SpaceObject20000-To-Madrid-DSS-34m - Times
SpaceObject20000-To-HBK-10m - Times
SpaceObject20000-To-GRGT-SGLR-16m - Times
SpaceObject20000-To-Goldstone-34m - Times
SpaceObject20000-To-Goldstone-70m - Times
SpaceObject20000-To-Canverra-70m - Times
SpaceObject20000-To-Canberra-34m - Times
SpaceObject20000-To-AUWA01-13m - Times
SpaceObject20000-To-ASF-11m - Times
SpaceObject20000-To-ASF-10m - Times
SpaceObject20000-To-AGO-12m - Times
12 Nov 2010 00:00:00.000
3:00
6:00
9:00
12:00
15:00
18:00
21:00
13 Sat
Time (UTCG)
12 Fri Nov 2010

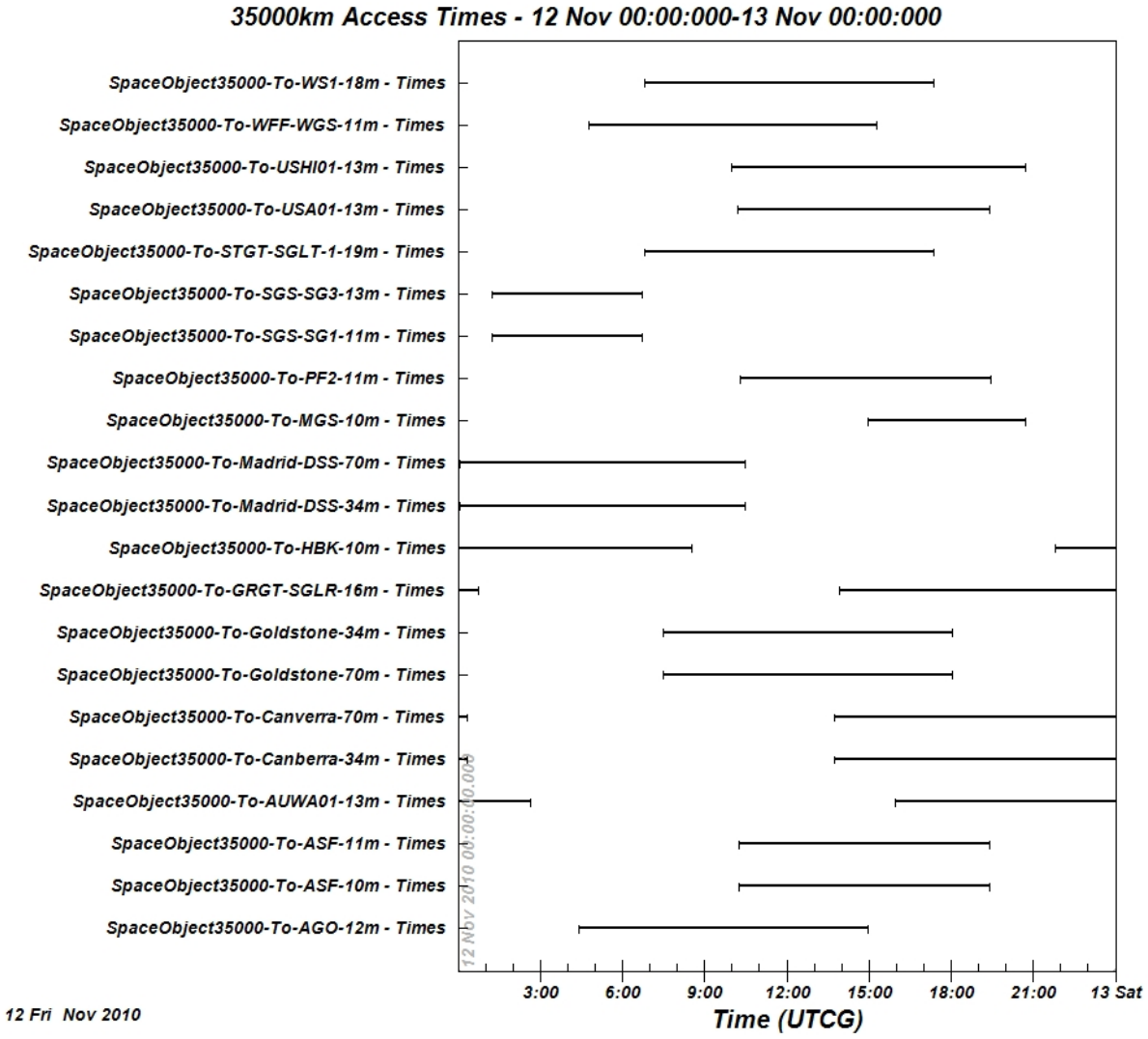
35000km Access Times - 12 Nov 00:00:000-13 Nov 00:00:000
SpaceObject35000-To-WS1-18m - Times
SpaceObject35000-To-WFF-WGS-11m - Times
SpaceObject35000-To-USHI01-13m - Times
SpaceObject35000-To-USA01-13m - Times
SpaceObject35000-To-STGT-SGLT-1-19m - Times
SpaceObject35000-To-SGS-SG3-13m - Times
SpaceObject35000-To-SGS-SG1-11m - Times
SpaceObject35000-To-PF2-11m - Times
SpaceObject35000-To-MGS-10m - Times
SpaceObject35000-To-Madrid-DSS-70m - Times
SpaceObject35000-To-Madrid-DSS-34m - Times
SpaceObject35000-To-HBK-10m - Times
SpaceObject35000-To-GRGT-SGLR-16m - Times
SpaceObject35000-To-Goldstone-34m - Times
SpaceObject35000-To-Goldstone-70m - Times
SpaceObject35000-To-Canverra-70m - Times
SpaceObject35000-To-Canberra-34m - Times
SpaceObject35000-To-AUWA01-13m - Times
SpaceObject35000-To-ASF-11m - Times
SpaceObject35000-To-ASF-10m - Times
SpaceObject35000-To-AGO-12m - Times
12 Nov 2010 00:00:00.000
3:00
6:00
9:00
12:00
15:00
18:00
21:00
13 Sat
Time (UTCG)
12 Fri Nov 2010

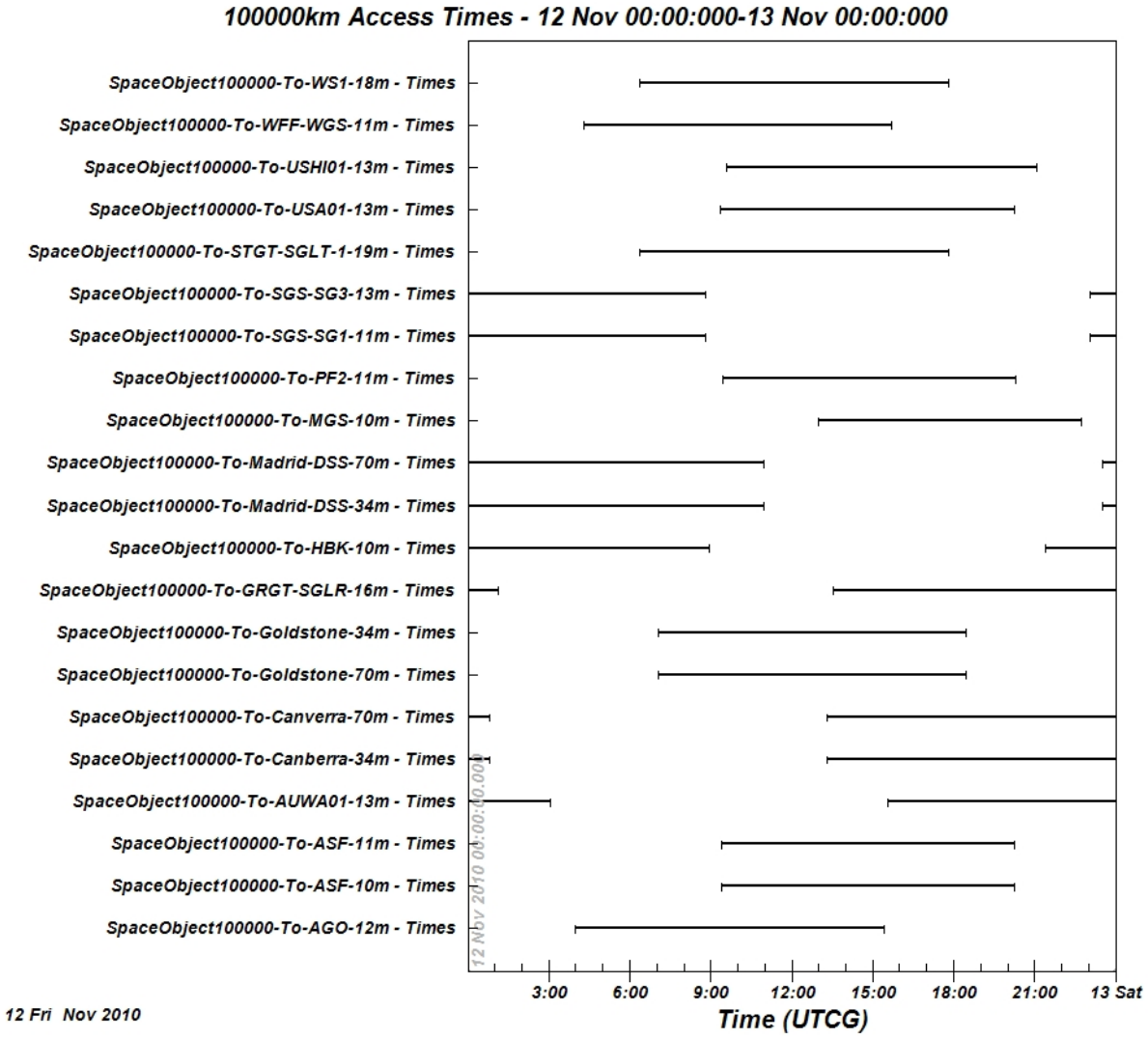
100000km Access Times - 12 Nov 00:00:000-13 Nov 00:00:000
SpaceObject100000-To-WS1-18m - Times
SpaceObject100000-To-WFF-WGS-11m - Times
SpaceObject100000-To-USHI01-13m - Times
SpaceObject100000-To-USA01-13m - Times
SpaceObject100000-To-STGT-SGLT-1-19m - Times
SpaceObject100000-To-SGS-SG3-13m - Times
SpaceObject100000-To-SGS-SG1-11m - Times
SpaceObject100000-To-PF2-11m - Times
SpaceObject100000-To-MGS-10m - Times
SpaceObject100000-To-Madrid-DSS-70m - Times
SpaceObject100000-To-Madrid-DSS-34m - Times
SpaceObject100000-To-HBK-10m - Times
SpaceObject100000-To-GRGT-SGLR-16m - Times
SpaceObject100000-To-Goldstone-34m - Times
SpaceObject100000-To-Goldstone-70m - Times
SpaceObject100000-To-Canverra-70m - Times
SpaceObject100000-To-Canberra-34m - Times
SpaceObject100000-To-AUWA01-13m - Times
SpaceObject100000-To-ASF-11m - Times
SpaceObject100000-To-ASF-10m - Times
SpaceObject100000-To-AGO-12m - Times
12 Nov 2010 00:00:00.000
3:00
6:00
9:00
12:00
15:00
18:00
21:00
13 Sat
Time (UTCG)
12 Fri Nov 2010

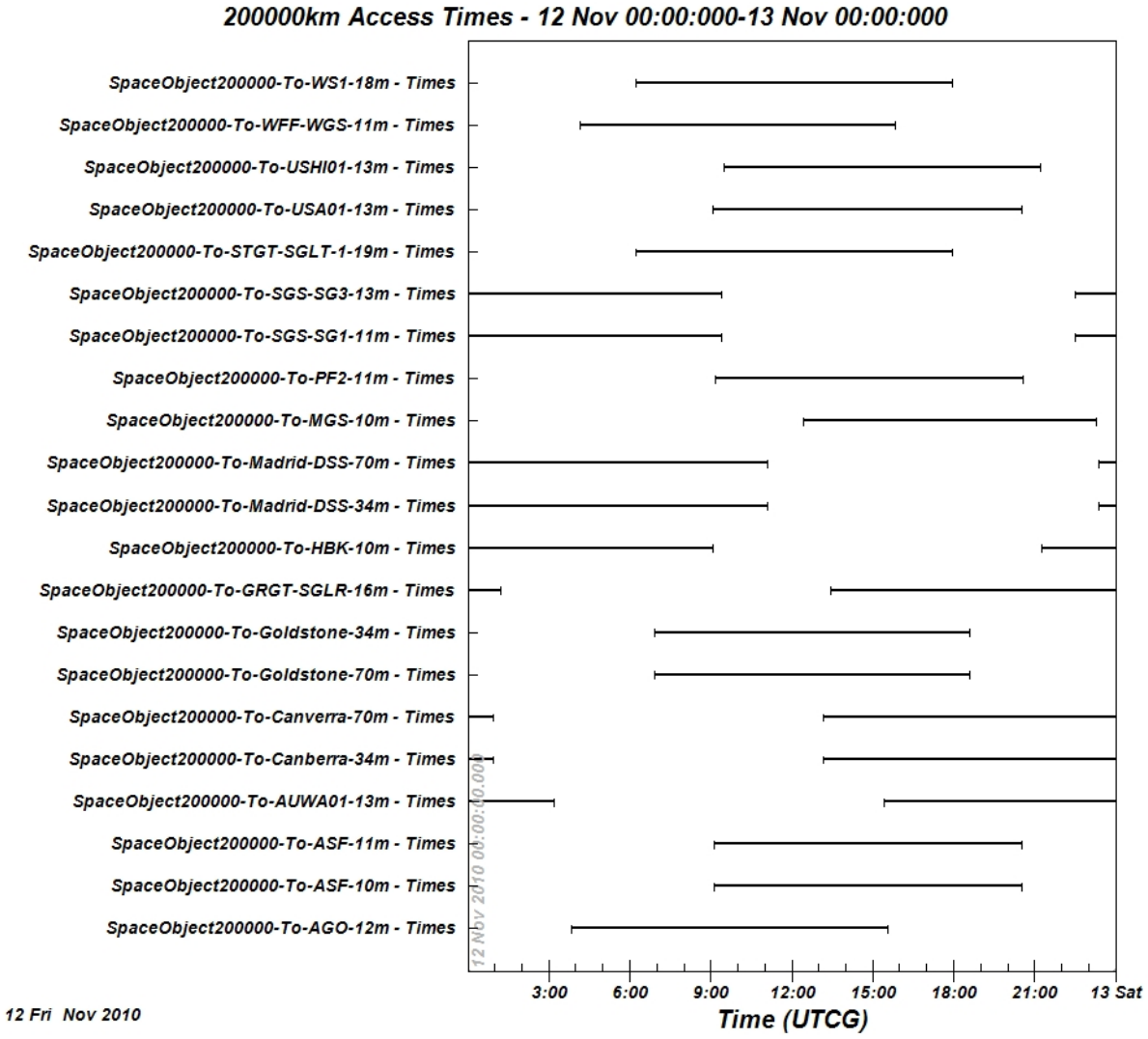
200000km Access Times - 12 Nov 00:00:000-13 Nov 00:00:000
SpaceObject200000-To-WS1-18m - Times
SpaceObject200000-To-WFF-WGS-11m - Times
SpaceObject200000-To-USHI01-13m - Times
SpaceObject200000-To-USA01-13m - Times
SpaceObject200000-To-STGT-SGLT-1-19m - Times
SpaceObject200000-To-SGS-SG3-13m - Times
SpaceObject200000-To-SGS-SG1-11m - Times
SpaceObject200000-To-PF2-11m - Times
SpaceObject200000-To-MGS-10m - Times
SpaceObject200000-To-Madrid-DSS-70m - Times
SpaceObject200000-To-Madrid-DSS-34m - Times
SpaceObject200000-To-HBK-10m - Times
SpaceObject200000-To-GRGT-SGLR-16m - Times
SpaceObject200000-To-Goldstone-34m - Times
SpaceObject200000-To-Goldstone-70m - Times
SpaceObject200000-To-Canverra-70m - Times
SpaceObject200000-To-Canberra-34m - Times
SpaceObject200000-To-AUWA01-13m - Times
SpaceObject200000-To-ASF-11m - Times
SpaceObject200000-To-ASF-10m - Times
SpaceObject200000-To-AGO-12m - Times
12 Nov 2010 00:00:10.000
3:00
6:00
9:00
12:00
15:00
18:00
21:00
13 Sat
Time (UTCG)
12 Fri Nov 2010

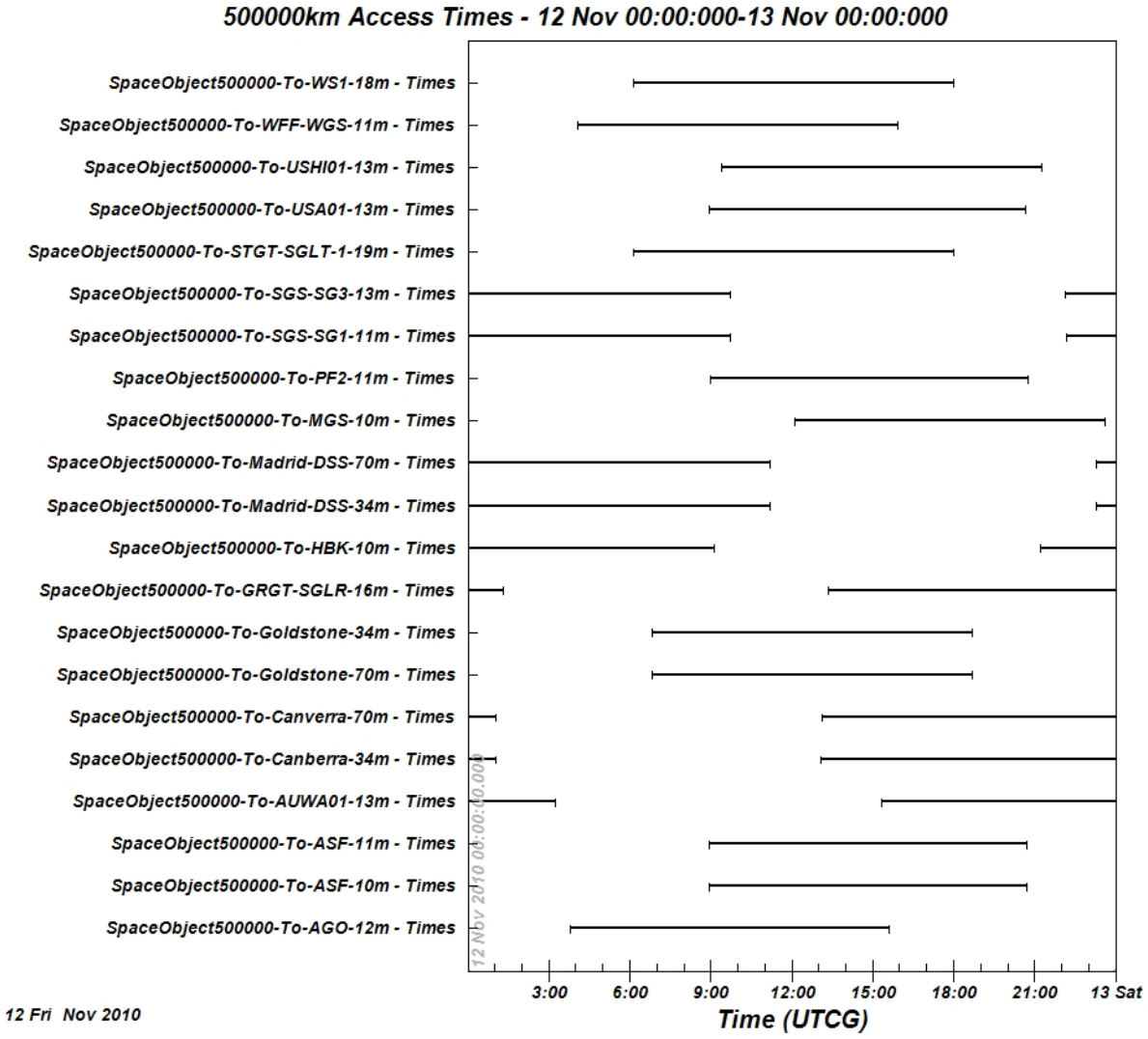
500000km Access Times - 12 Nov 00:00:000-13 Nov 00:00:000
SpaceObject500000-To-WS1-18m - Times
SpaceObject500000-To-WFF-WGS-11m - Times
SpaceObject500000-To-USHI01-13m - Times
SpaceObject500000-To-USA01-13m - Times
SpaceObject500000-To-STGT-SGLT-1-19m - Times
SpaceObject500000-To-SGS-SG3-13m - Times
SpaceObject500000-To-SGS-SG1-11m - Times
SpaceObject500000-To-PF2-11m - Times
SpaceObject500000-To-MGS-10m - Times
SpaceObject500000-To-Madrid-DSS-70m - Times
SpaceObject500000-To-Madrid-DSS-34m - Times
SpaceObject500000-To-HBK-10m - Times
SpaceObject500000-To-GRGT-SGLR-16m - Times
SpaceObject500000-To-Goldstone-34m - Times
SpaceObject500000-To-Goldstone-70m - Times
SpaceObject500000-To-Canverra-70m - Times
SpaceObject500000-To-Canberra-34m - Times
SpaceObject500000-To-AUWA01-13m - Times
SpaceObject500000-To-ASF-11m - Times
SpaceObject500000-To-ASF-10m - Times
SpaceObject500000-To-AGO-12m - Times
12 Nov 2010 00:00:10.000
3:00
6:00
9:00
12:00
15:00
18:00
21:00
13 Sat
Time (UTCG)
12 Fri Nov 2010

REPORT DOCUMENTATION PAGE	Form Approved OMB No. 0704-0188

1. REPORT DATE *(DD-MM-YYYY)*	2. REPORT TYPE	3. DATES COVERED *(From - To)*
01-05-2012	Technical Memorandum	

4. TITLE AND SUBTITLE
Performance Analysis of a NASA Integrated Network Array

5a. CONTRACT NUMBER

5b. GRANT NUMBER

5c. PROGRAM ELEMENT NUMBER

6. AUTHOR(S)
Nessel, James, A.

5d. PROJECT NUMBER

5e. TASK NUMBER

5f. WORK UNIT NUMBER
WBS 439432.04.04.07

7. PERFORMING ORGANIZATION NAME(S) AND ADDRESS(ES)
National Aeronautics and Space Administration
John H. Glenn Research Center at Lewis Field
Cleveland, Ohio 44135-3191

8. PERFORMING ORGANIZATION REPORT NUMBER
E-17788

9. SPONSORING/MONITORING AGENCY NAME(S) AND ADDRESS(ES)
National Aeronautics and Space Administration
Washington, DC 20546-0001

10. SPONSORING/MONITOR'S ACRONYM(S)
NASA

11. SPONSORING/MONITORING REPORT NUMBER
NASA/TM-2012-217112

12. DISTRIBUTION/AVAILABILITY STATEMENT
Unclassified-Unlimited
Subject Category: 32
Available electronically at http://www.sti.nasa.gov
This publication is available from the NASA Center for AeroSpace Information, 443-757-5802

13. SUPPLEMENTARY NOTES

14. ABSTRACT
The Space Communications and Navigation (SCaN) Program is planning to integrate its individual networks into a unified network which will function as a single entity to provide services to user missions. This integrated network architecture is expected to provide SCaN customers with the capabilities to seamlessly use any of the available SCaN assets to support their missions to efficiently meet the collective needs of Agency missions. One potential optimal application of these assets, based on this envisioned architecture, is that of arraying across existing networks to significantly enhance data rates and/or link availabilities. As such, this document provides an analysis of the transmit and receive performance of a proposed SCaN inter-network antenna array. From the study, it is determined that a fully integrated inter-network array does not provide any significant advantage over an intra-network array, one in which the assets of an individual network are arrayed for enhanced performance. Therefore, it is the recommendation of this study that NASA proceed with an arraying concept, with a fundamental focus on a network-centric arraying.

15. SUBJECT TERMS
Array; Deep space network; Near Earth network; Space network

16. SECURITY CLASSIFICATION OF:			17. LIMITATION OF ABSTRACT	18. NUMBER OF PAGES	19a. NAME OF RESPONSIBLE PERSON
a. REPORT	b. ABSTRACT	c. THIS PAGE			STI Help Desk (email:help@sti.nasa.gov)
U	U	U	UU	42	19b. TELEPHONE NUMBER *(include area code)* 443-757-5802